PROGRESS REPORT
Grant NGL 34-002-047
October 15, 1970

"STUDY OF RECTANGULAR-GUIDE-LIKE STRUCTURES FOR MILLIMETER WAVE TRANSMISSION"

to
The National Aeronautics and Space Administration, Washington, D. C.

DEPARTMENT OF ELECTRICAL ENGINEERING
NORTH CAROLINA STATE UNIVERSITY
RALEIGH, NORTH CAROLINA

PROGRESS REPORT
Grant NGL 34-002-047
October 15, 1970

"STUDY OF RECTANGULAR-GUIDE-LIKE STRUCTURES FOR MILLIMETER WAVE TRANSMISSION"

to
The National Aeronautics and Space Administration, Washington, D. C.

North Carolina State University
Raleigh, North Carolina

Submitted: Frederick J. Tischer

Dr. Frederick J. Tischer, Professor
Principal Investigator

PERSONNEL

Dr. Frederick J. Tischer, Principal Investigator

Mr. Lyles Adair, Graduate Student

Mr. K. K. Agarwal, Graduate Student

Mr. F. Jalali, Graduate Student

Mr. R. A. Kraft, Graduate Student

Mr. J. R. Potukuchi, Graduate Student

TABLE OF CONTENTS

INTRODUCTION

This progress report presents results of research carried out under Grant NGL 34-002-047 during the period June 1, 1970 to September 30, 1970.

During the report period an extensive measurement program was carried out since the equipment assembled and in part developed during preceding periods became operational in a condition to yield the desired and necessary high-accuracy data.

The equipment for the measurement of electromagnetic fields equipped with a plotter and compensated probes permits accurate and effective determination of field distributions inside and outside of open waveguides and resonators. The effects of the probes on the measured field distributions have been studied, are known, and can be reduced in part by the choice of proper locations for the measurements and in part by compensation.

The error of the setup for the Q-value measurements has been reduced during the last year by about a factor 5. The setup facilitates measurements with an accuracy of about $\pm$ 1% using routine procedures and better under special conditions. It can be used for frequencies up to 100 GHz. The improvement was necessary to give reliable data for the comparative study of various approaches for non-conventional methods of transmission of millimeter waves and for the determination of the effects of surface properties, such as roughness, on the attenuation of waveguides and on the Q-value of

resonators.

A comparative study of the field distributions of two prototypes of fence guides are described in part 1 of the report. The two models differ by the spacing between the wires of the wire grids forming the side walls. Longitudinal distributions of the fields were measured under various conditions of loading by dielectric slabs and for different conditions of loading by the probe at a series of frequencies. The data were then evaluated to give the guide wavelength. Transverse field distributions inside and outside and the vertical decay of the field inside the guide were measured also. The data were evaluated and the results gave valuable information for the design of fence guides. During these measurements, the effects of loading by the probe were studied. As a result of this study measurement procedures were developed for reducing the effects of probe loading.

The two sections of fence guide were then used as resonators for the determination of the Q-values. The Q-values in turn permit finding the values of attenuation of the guides. This study is described in part 2 of the report. It was found that due to nonuniformity of the fence guide, measurements of the attenuation by evaluation of the Q-value give more reliable results than other possible measurements. The study was then extended to test the effect of loading the fence guide by additional dielectric slabs in the center of the guide. It was found that the Q-values became considerably higher in the case of loading, as it was anticipated. Q-values

as high as 2000 were measured. This compares with values of about 800 for the unloaded fence guide. The loading was carried out by adding a dielectric strip 1/32" thick on top of the regular dielectric slab between the fences of the guide.

Part 3 of the report presents the results of an investigation of parallel-wall waveguides with various cross-sectional geometries for dielectric loading. The effects of placing dielectric strips oriented parallel and perpendicular to the side walls and circular rods in the parallel-wall waveguide were investigated. Longitudinal and transverse field distributions and Q-values of shorted sections of the loaded guides were measured and evaluated. Rexolite and Lucalox (a high-purity alumina oxide) were used as dielectrics. The results of these measurements can be used to obtain optimum cross-sectional geometries for H-guides and loaded fence guides. It was observed that the attenuation of fence guides can be reduced by dielectric loading, which means by adding a dielectric strip or rod to the central dielectric slab. Evaluation of the results suggests optimum structures for the loading.

Preliminary results of the study of surface roughness on the Q-value of resonators and on the attenuation of waveguides are described in part 4. The millimeter-wave and optical equipment of the laboratory and the developed measurement procedures made such a study possible. Its task is the analysis of discrepancies observed between the experimental and theoretical values of the quality factors of resonators

and of the attenuations of waveguides at very high frequencies. Discrepancies of about 30% are common in the frequency region at around 35 GHz. The effects of surface roughness are measured electrically and correlated with the surface structures observed mechanically and optically. The H-guide cavity used for these measurements eliminates difficulties encountered at similar measurements using customary cavities.

Part 5 of this report deals with a study of microstrip lines in the frequency range of about 32 to 36 GHz. A literature review carried out previously, the evaluation of data presented at professional meetings, and discussions with researchers working in this area, showed that it is difficult to obtain reliable data of these lines in this frequency range. Results of measurements carried out in different laboratories and by different people do not agree. Since reliable data are required for a comparison of nonconventional transmission methods and since equipment and procedures for accurate measurements are available in our laboratory, measurements were initiated to find the characteristics of a number of samples of commercially available striplines. A measurement setup with transitions from waveguides to striplines was prepared and measurements carried out. It became apparent in the early stages of the measurements that they are difficult to carry out and that it is similarly difficult to obtain repeatable and reliable results. The measurements were then extended to be made according to three different methods.

measurements on transmission-type cavities made of sections of microstrip, and (3) Q-value measurements of resonant sections by evaluation of input reflection coefficients. The measurement procedures were continuously improved until agreement of the results was obtained. It was found that contact problems, secondary radiation from the transitions, and spurious wave modes considerably affected the measurements. Only by careful operations could these difficulties be overcome. It is felt that the measured data presented in part 5 of this report have been obtained by such operations and have the desired reliability. They can be used in the comparison of nonconventional methods of millimeter wave transmission.

At present, an attempt is being made to extend the fence guide concept toward lower frequencies, namely 15 GHz. The work will yield desired data for circuits based on this concept and it will indicate the lower frequency limit of the application of this concept.

COMPARATIVE STUDY OF FENCE-GUIDE FIELDS

Abstract

Measurements were carried out on two prototypes of fence guide with slightly different spacings between the posts of the wire grids forming the sidewalls. The field distributions inside and in the vicinity of the guide were determined. Their evaluation gives the values of the guide wavelength and of the decay factors for the exponential field decrease above and below the dielectric slab. Loading effects due to the probe were investigated and attempts made to correct the measured results and to eliminate errors due to loading. The loading effect of the probe was found to cause double peaks of the field distributions. A brief description of the loading and the compensation is included in the appendix.

A COMPARATIVE STUDY OF FENCE-GUIDE FIELDS

Introduction

Measurements of electromagnetic fields carried out on a fence guide were reported in the progress report (NGL 34-002-047). Additional and more detailed measurements were carried out on two 175 mm long sections of fence guide to study the effects of the spacing of wires of the fence. The prototype fence guides were fabricated using copper wires of diameter d_w = 0.862 mm and spacings s_w = 1.168 mm (Model II) and 1.016 mm (Model I) on a Rexolite sheet of 1/32" thickness. Experimental efforts were made to determine:

(1) Longitudinal distributions of field under various load conditions.

(2) Guide wavelength, λ_g, as a function of frequency.

(3) Transverse field distributions inside the fence guide, taking into consideration loading by the probe.

(4) Exponential decay of the transverse field.

The effects of probes on the field distribution were preliminarily studied and a brief description is included in the appendix.

The measurements were made using an improved capacitive monopole with compensation. The diameter of the probe was reduced to 1.70 mm in combination with a coaxial cable of 0.82 mm. It was found that the probe affects the field distribution appreciably. When used to measure the fields, the probe loaded the waveguide causing a reduction of the output power of the fence guide by as much as 10-12 db in the strong-field region to little or no (about 0.5 db) loading at very low field=

strength values. Curves showing the amount of loading are included. In some cases, the curves were compensated for the loading effect.

Longitudinal Distribution

The field distribution in the longitudinal direction was measured under short-circuit and matched-load conditions. They were determined at the center, at two different heights and near the fence wires. The curves showing the measurement results are displayed in Figs. 1 to 7 .

The short-circuit standing-wave patterns as reported in the earlier report NGL 34-002-047 of June 15, 1970 and as shown in Fig. 1 and Fig. 4 for the two fence guide models at 1 mm above the dielectric, have some maxima with double peaks. The measurements were repeated at 5 mm above the dielectric where the field is about 6 db lower than at 1 mm due to the exponential decay. The resulting field distribution plotted in Fig. 2 has no double peaks. Standing wave distributions near the fence (inside) at 1 mm above the dielectric with one shown in Fig. 5a and 5b also have no double peaks. The field near the fence is rather low due to the sinusoidal variation of the transverse field, and this results in a lower loading effect. This then shows that double-peaks are primarily the result of loading by the probe.

Longitudinal field distribution with a matched load (TRG-VSWR 1.05) are shown in Fig. 6 to Fig. 7 at 1 mm and 5 mm above the dielectric. The patterns are irregular and the maximum VSWR varies from 3 db to 5 db. The power levels being

Fig. 1 Longitudinal Distribution, Model I .
F = 35.04 GHz, center, 1mm above

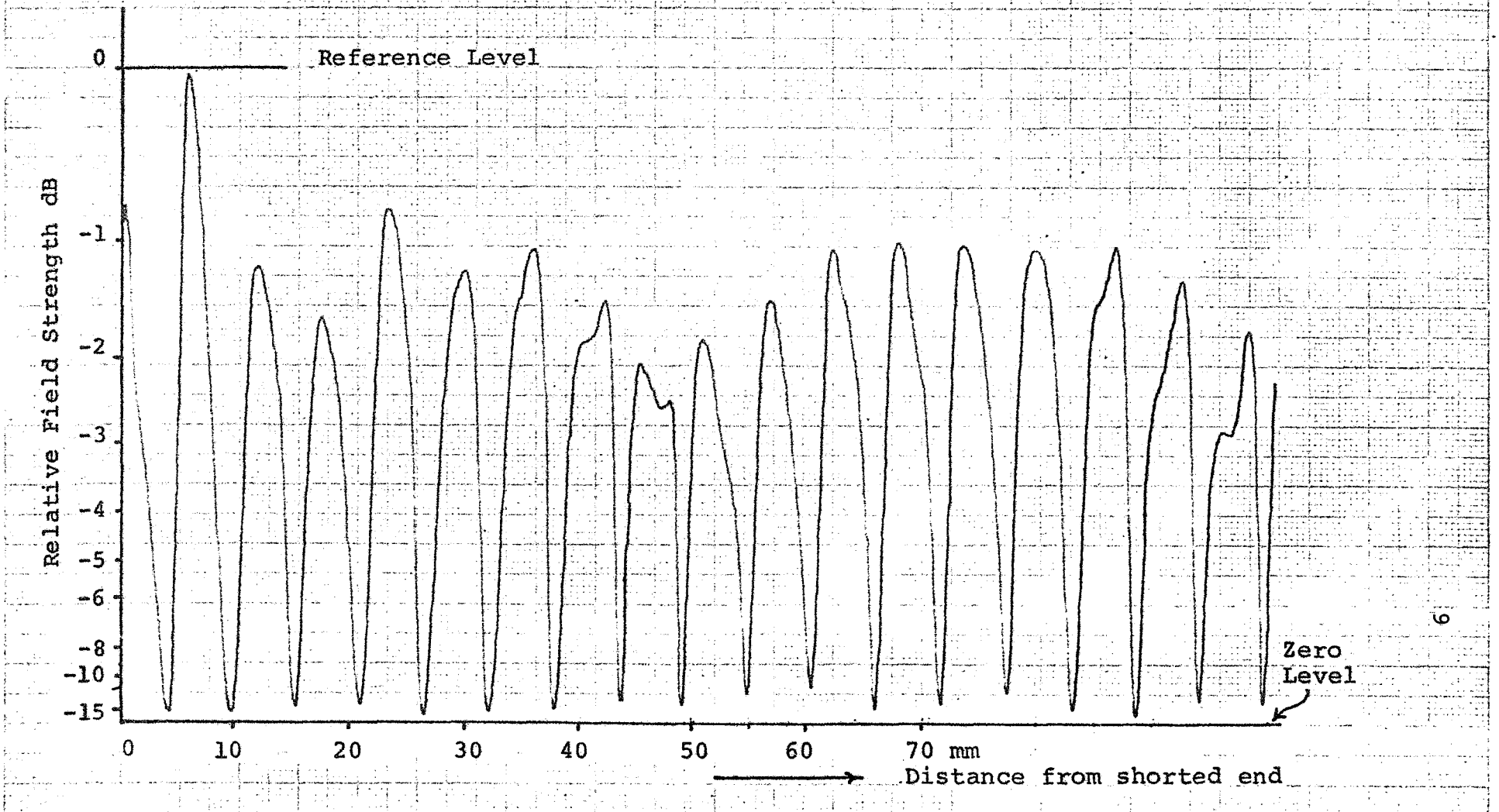

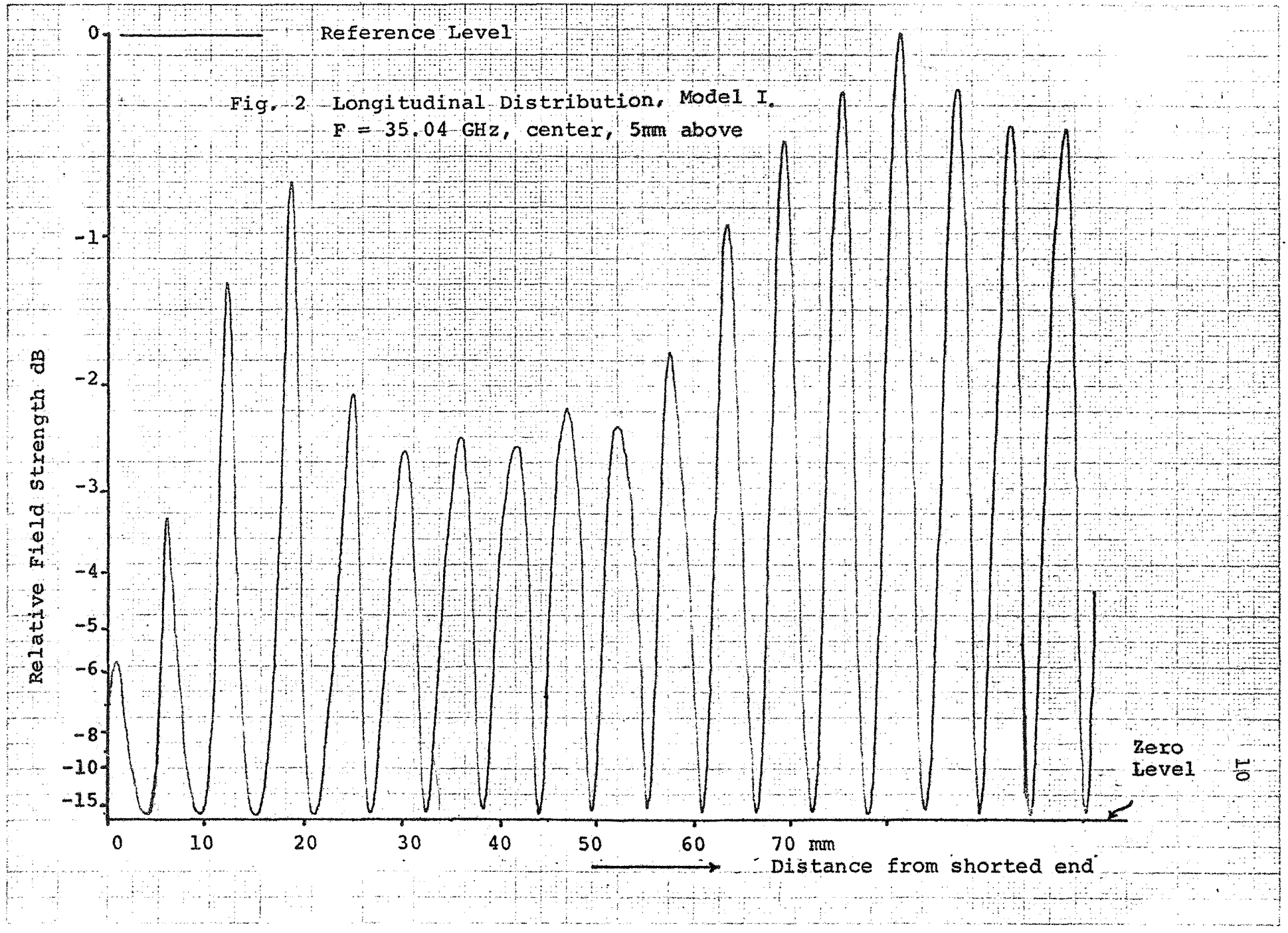
Reference Level
Fig. 2 Longitudinal Distribution, Model I.
F = 35.04 GHz, center, 5mm above
0
-1
-2
-3
-4
-5
-6
-8
-10
-15
Relative Field Strength dB
Zero Level
10
0
10
20
30
40
50
60
70 mm
Distance from shorted end

Fig. 3 Output Power of Guide (Loading Effect).
Model I, F = 35.04 GHz, center, 5 mm above

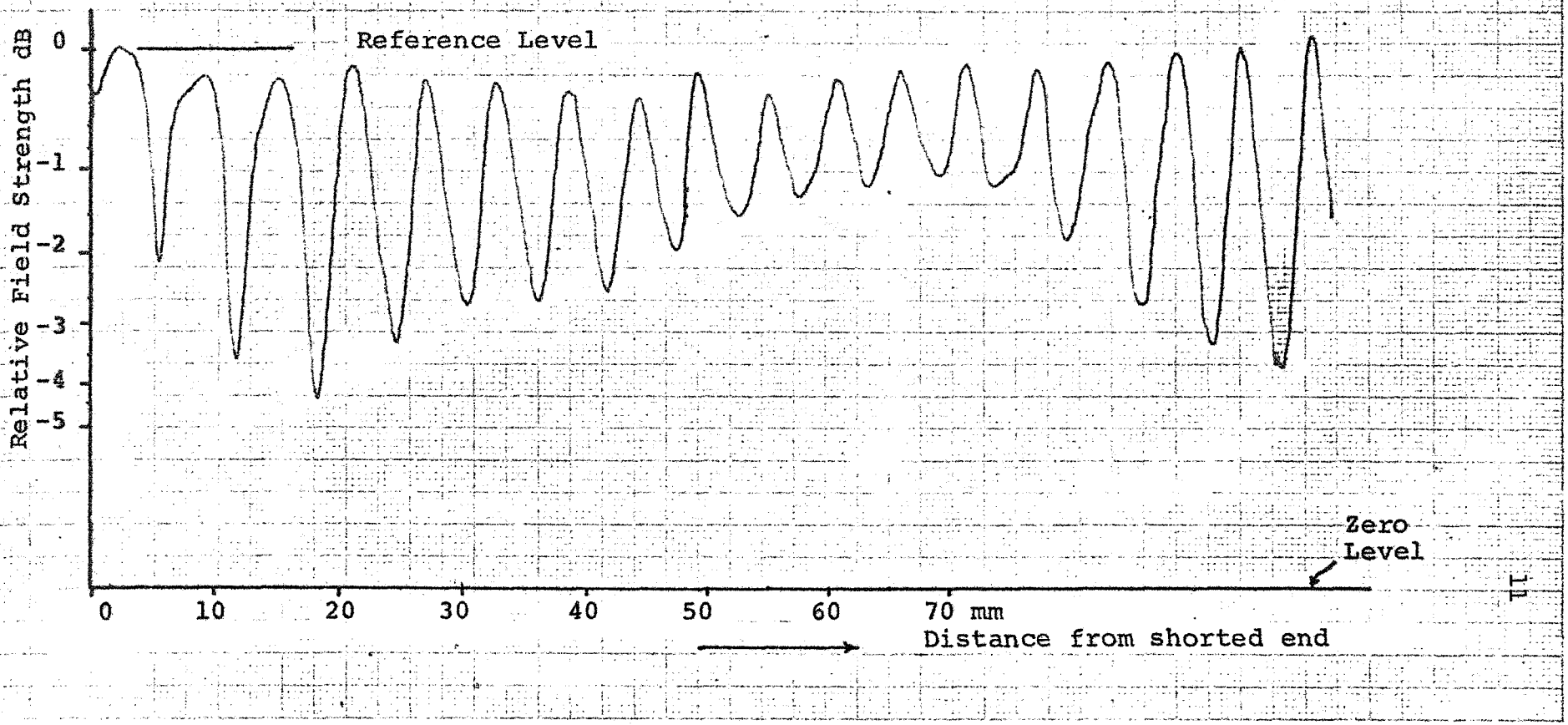

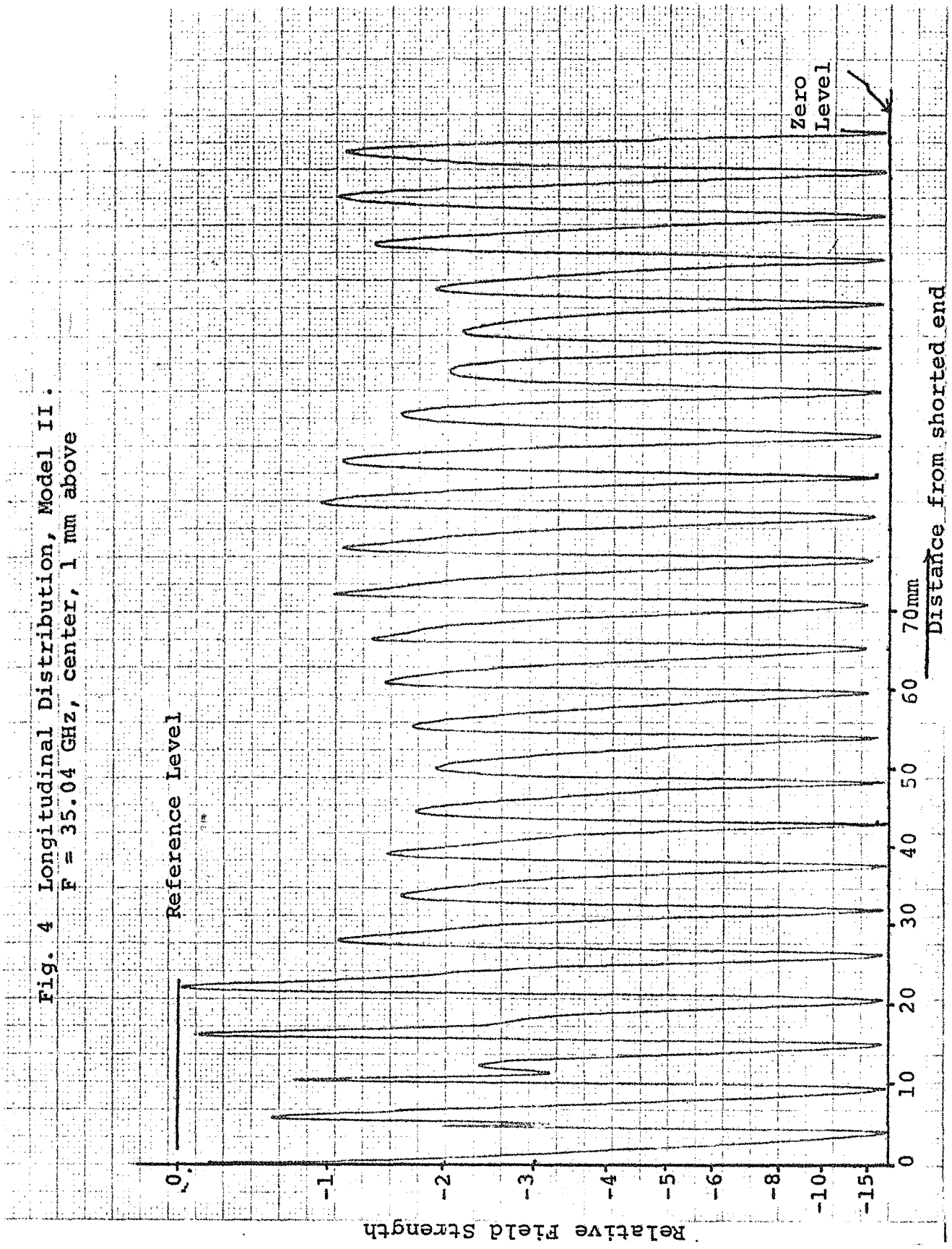

Fig. 4 Longitudinal Distribution, Model II.
F = 35.04 GHz, center, 1 mm above

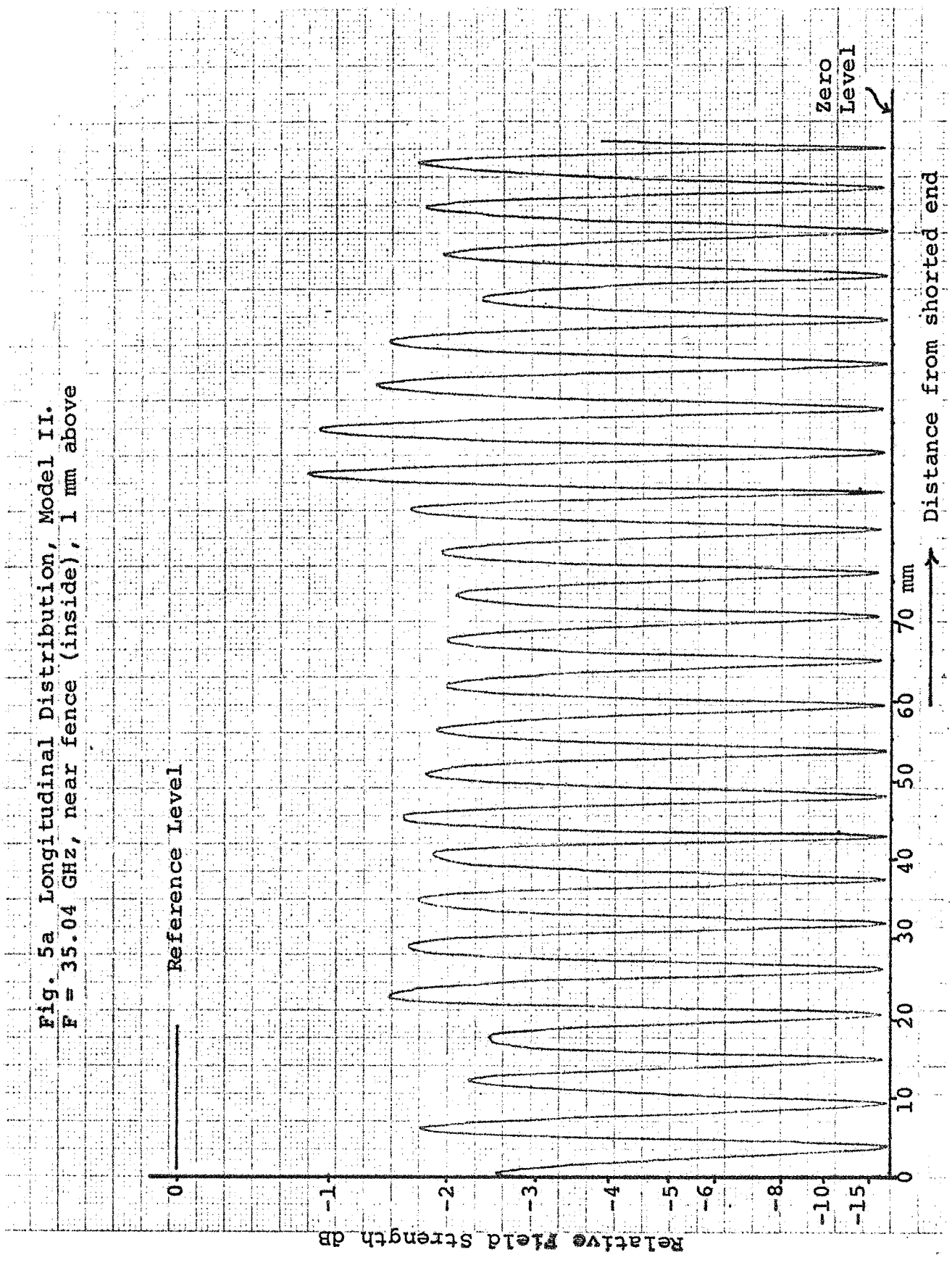

Fig. 5a Longitudinal Distribution, Model II.
F = 35.04 GHz, near fence (inside), 1 mm above

Fig. 5b Longitudinal Distribution, Model I.
F = 35.04 GHz, near fence (inside), 1 mm above

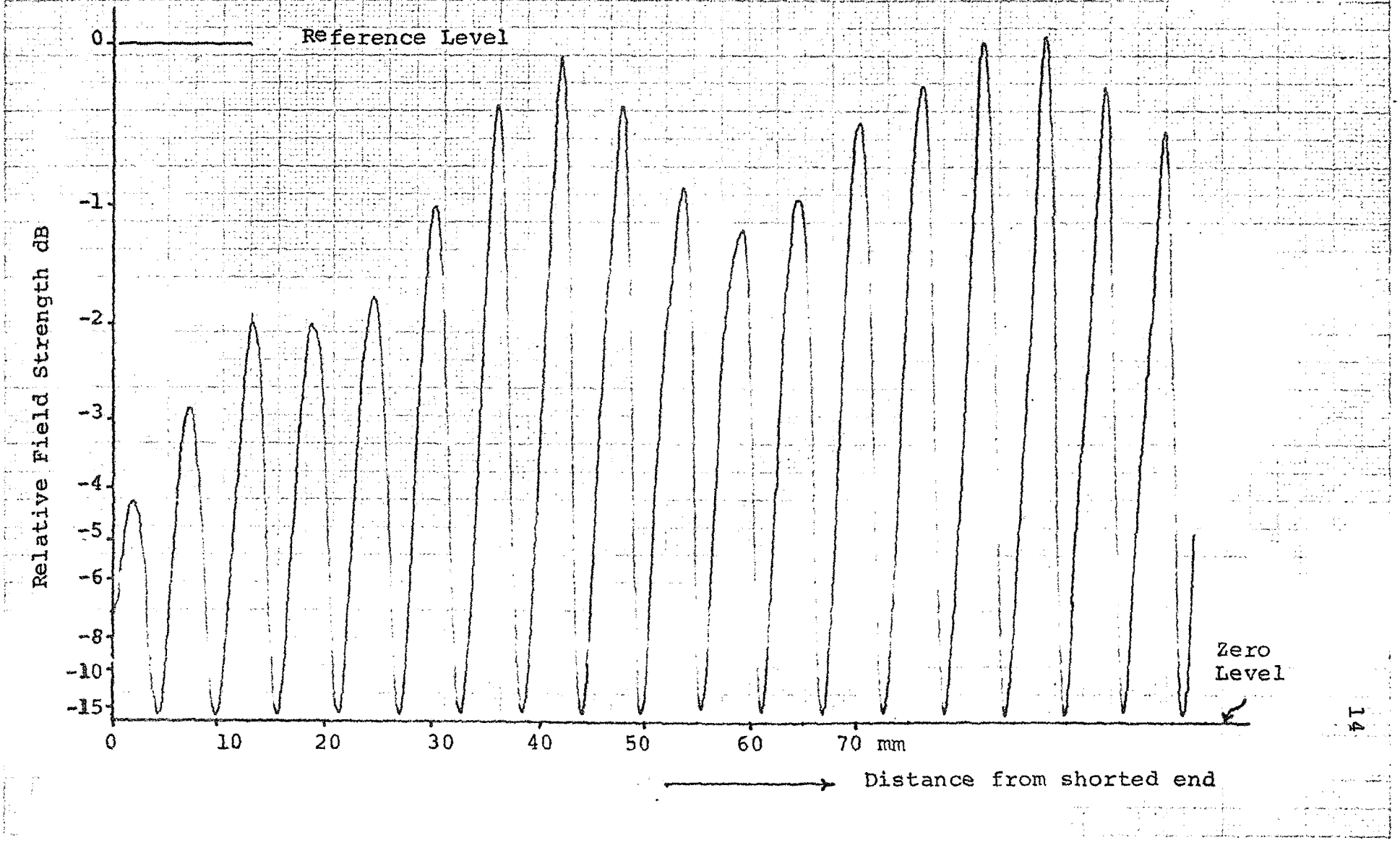

Fig. 6 Distribution for Low Reflections, Model 1.

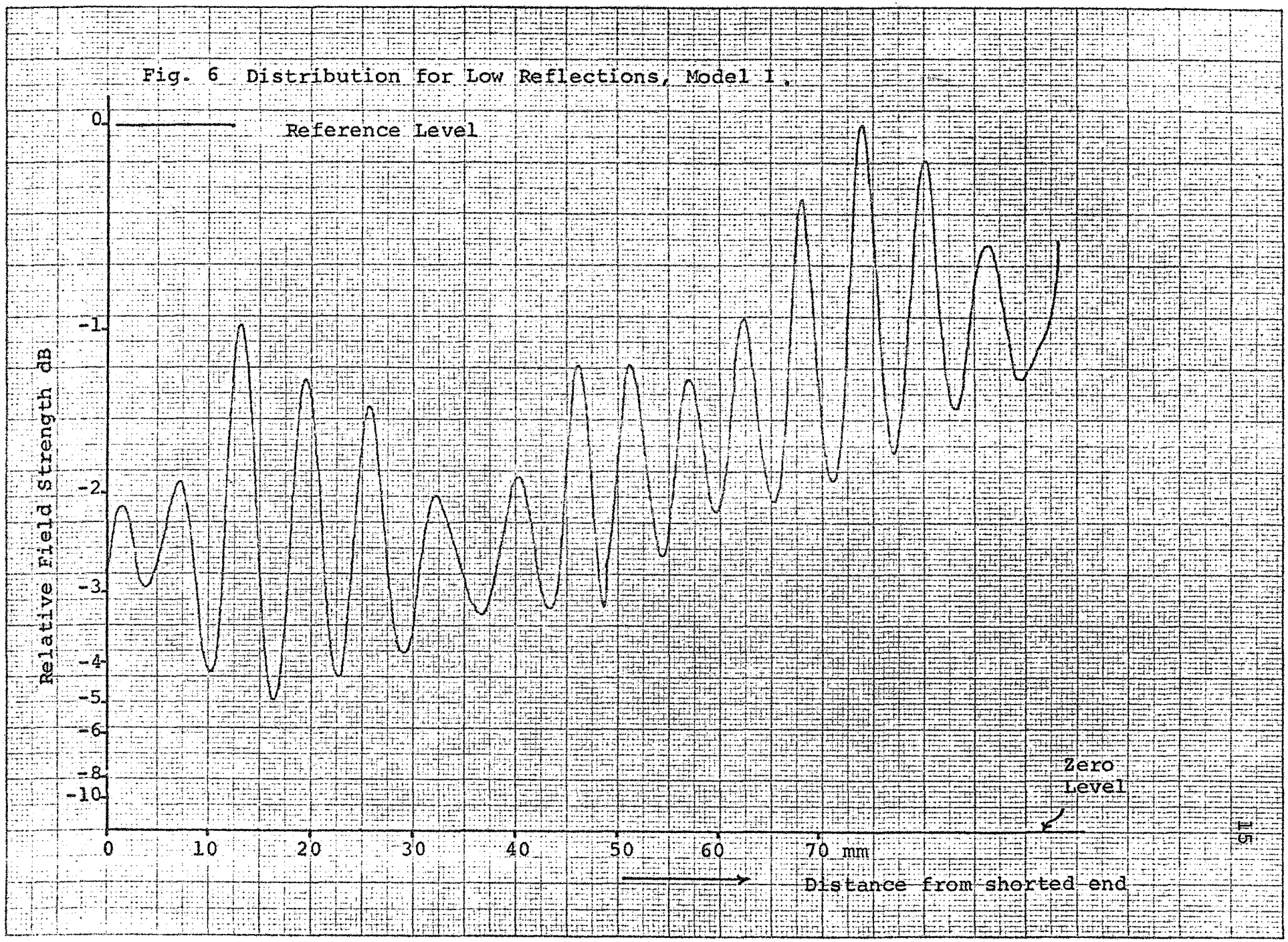

Fig. 7 Distribution for Low Reflections, Model II.

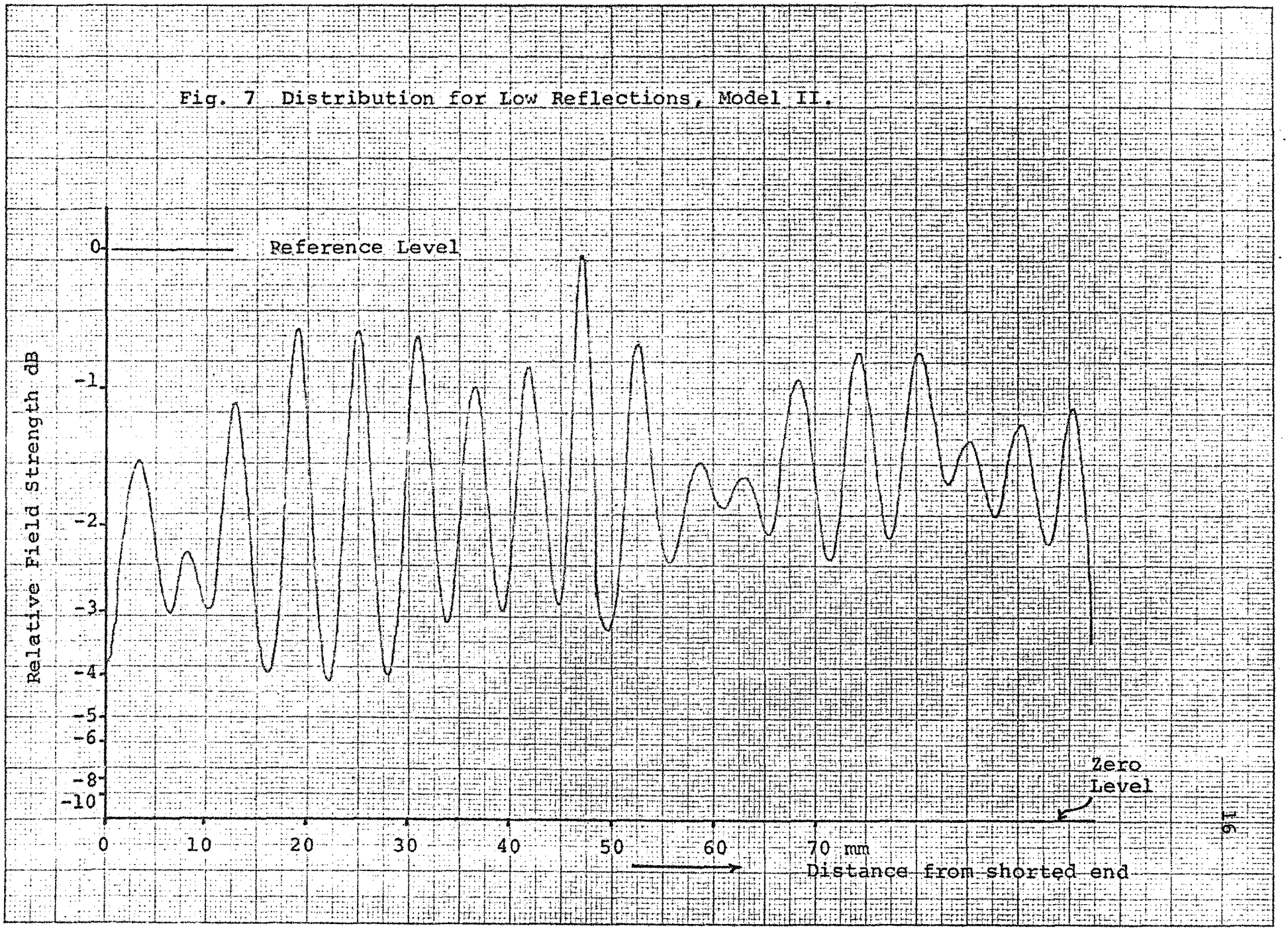

Fig. 8 Distribution Inside and Outside the Guide.
(Model I, s_w = 1.016 mm)
A: Inside
B: Outside

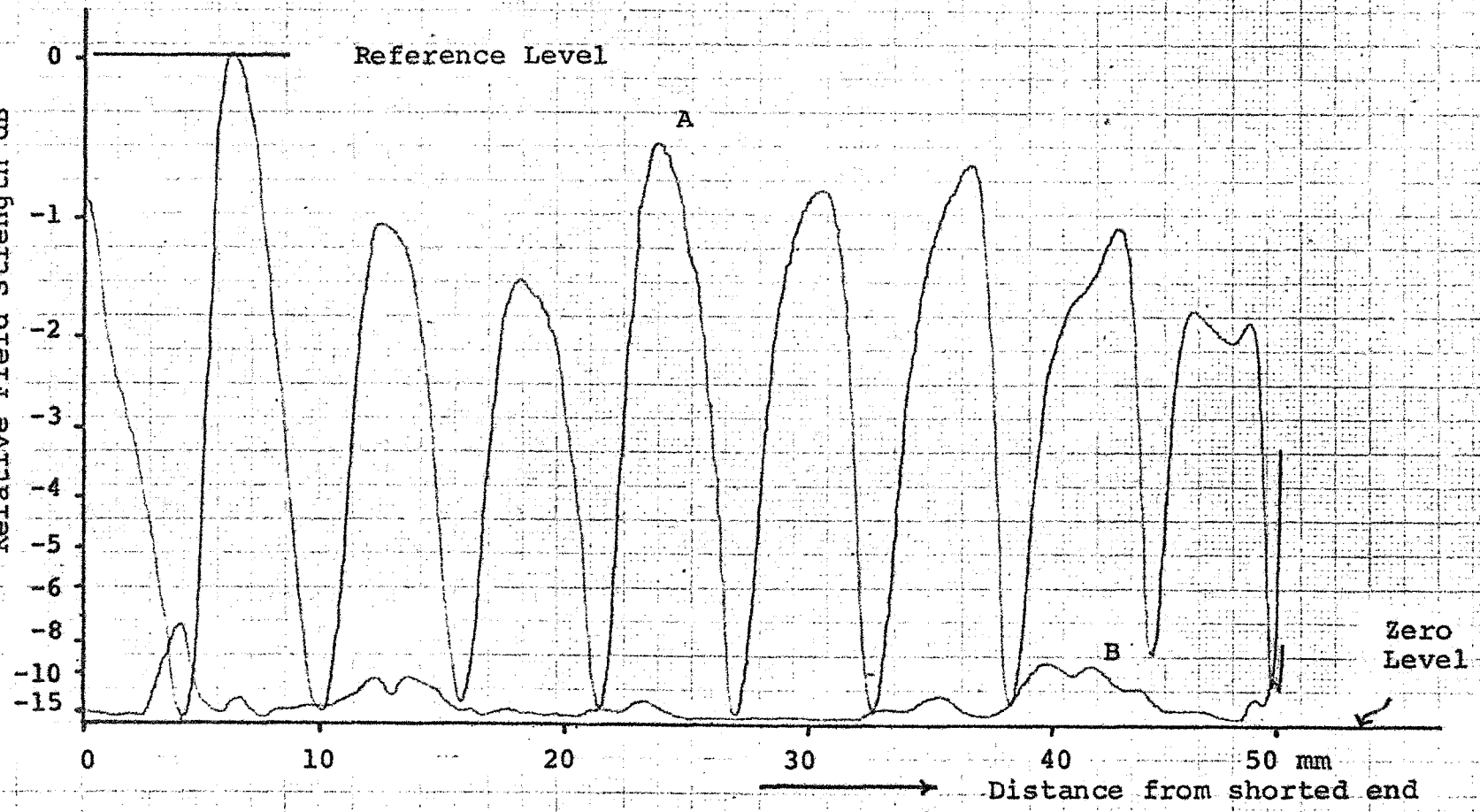

considerably lower, the patterns have no double peaks.

The relative magnitude of the field outside the fence is also of interest. The fields were measured inside at the center and outside at 3 mm away from the fence, with the guide shorted at the end. The plots are Fig. 8 and 9. One observes that the outside field is at least 36 db below the maximum field inside in both fence guides. This indicates that leakage is not very much affected by small changes in fence spacing.

Guide Wavelength

The longitudinal standing wave patterns were measured in the frequency range 34.5 - 37.0 GHz at 0.5 GHz interval for the two fence guides and guide wavelengths at these frequencies were computed.

Table I

Frequency GHz	λ_g in mm for fence guide with spacing	
	S_w = 1.016 mm	S_w = 1.168 mm
34.5	11.46959	11.54954
35.0	11.17648	11.20720
35.5	10.96283	10.95495
36.0	10.63593	10.64189
36.5	10.38155	10.33783
37.0	10.13513	10.09804

Fig. 10 is a plot of Table I for the two fence guides and shows that the variation of the guide wavelength with frequency is fairly close to a straight line (slope 0.53 mm/GHz). The two curves differ by a maximum deviation of 0.07995, of measurement as well as any effects of change of spacing on guide wavelength.

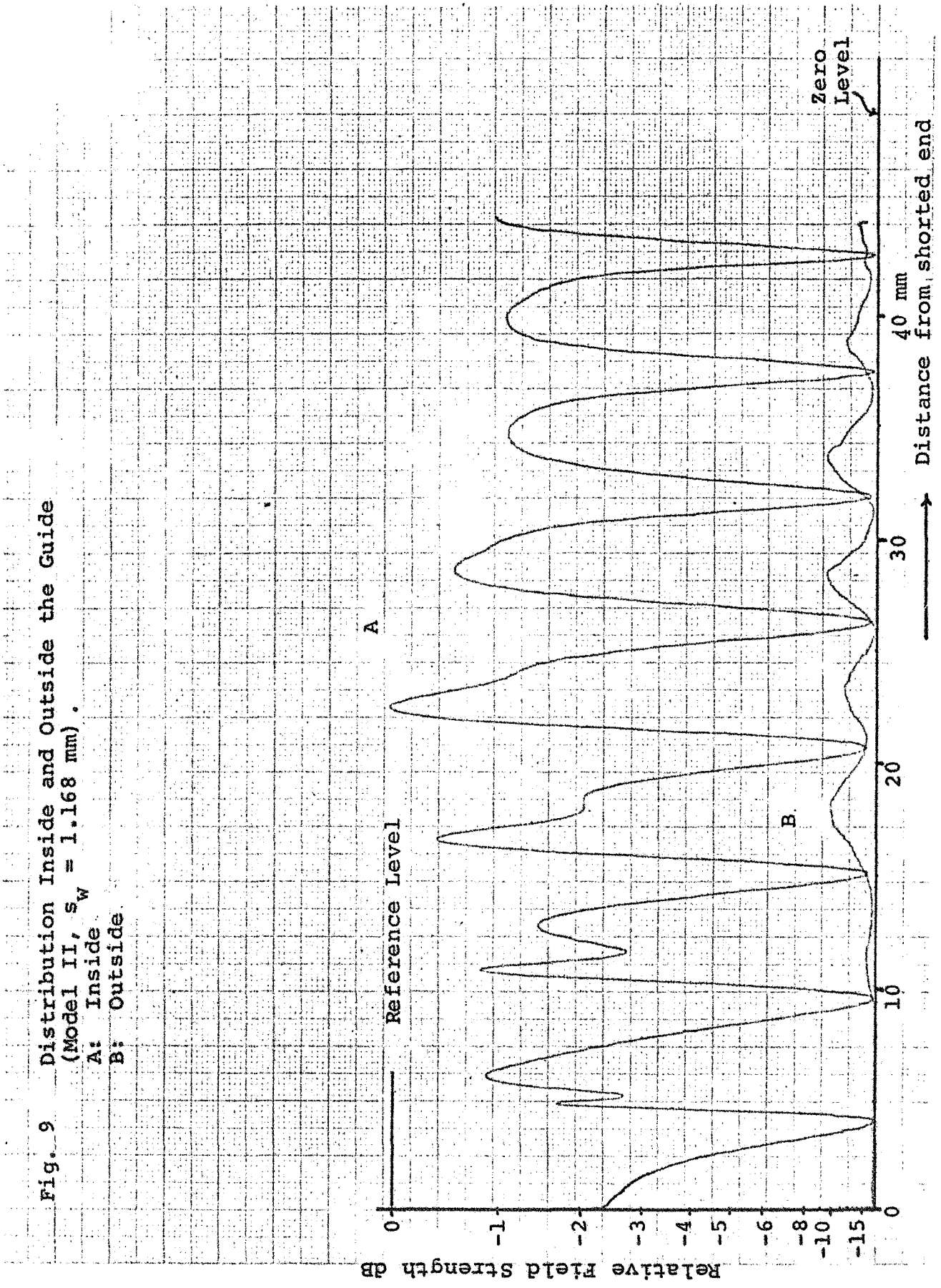

Fig. 9 Distribution Inside and Outside the Guide (Model II, s_w = 1.168 mm).
A: Inside
B: Outside

Fig. 10 Variation of Guide Wavelength with Frequency in Fence Guides.
A: Model I (s_w = 1.016 mm).
B: Model II (s_w = 1.168 mm).

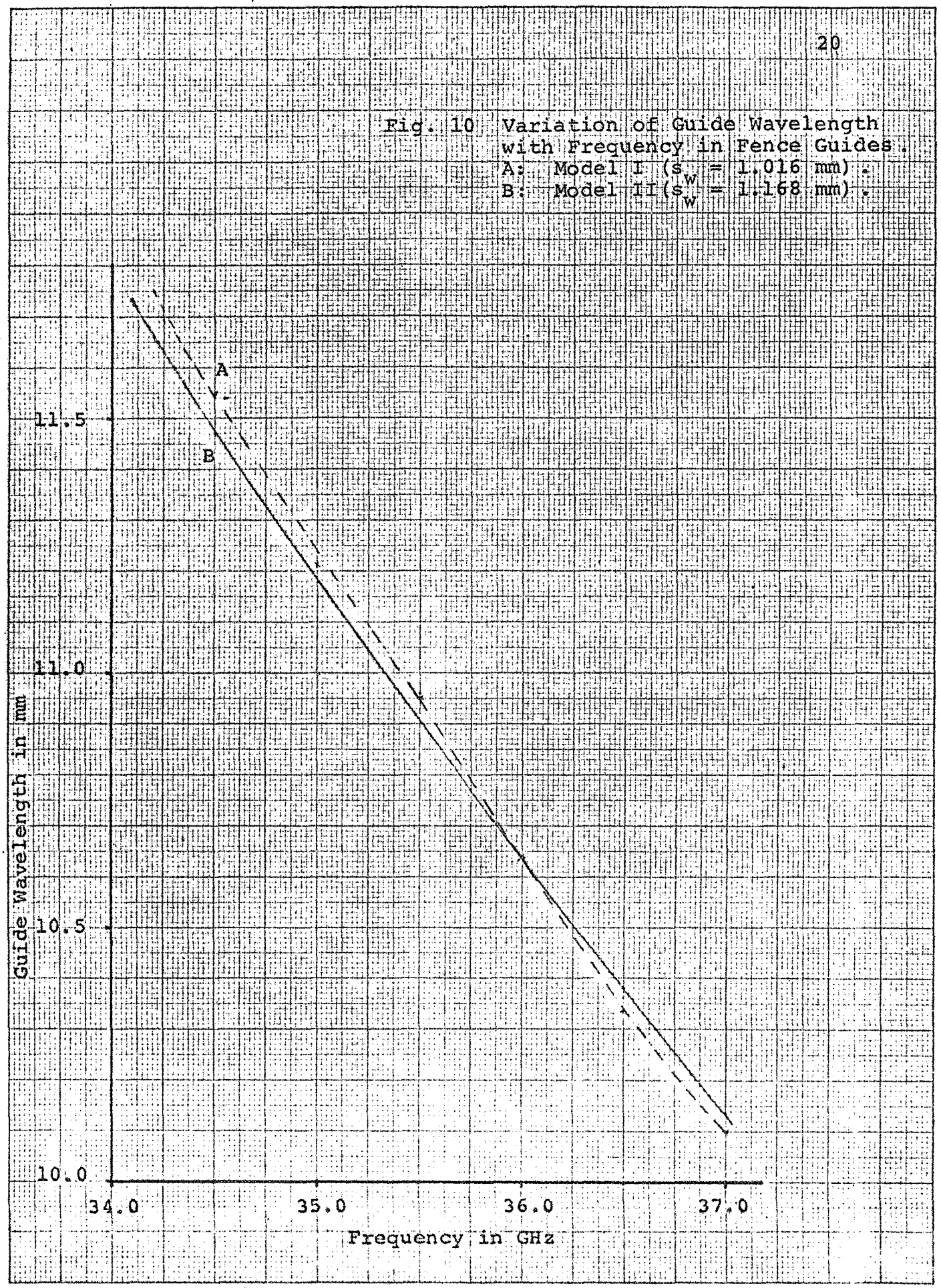

Transverse-Field Distributions

Transverse-field measurements were carried out at the location of various maxima at different heights. Fig. 11 shows plots in the fourth maximum of the field distribution and the guide output. The distributions have the double peaks. A plot of the compensated field distribution at 2 mm height is shown in Fig. 12. The effect of loading can be clearly seen with compensation, the double peak vanishes, the distribution is close to sinusoidal.

Transverse fields measured above the level of the fence are shown in Fig. 13 for different heights in steps of 5 mm. The field is very symmetrical with respect to the fence guide center where it is maximum. The loading due to probe was negligibly small due to the field being more than 15 db below the field at the 1 mm level above the dielectric. The figures also include a plot of the maximum field versus height. The rate of field decrease for the two fence guides are:

Table II

Fence guide with spacing (mm)	Field decrease in db/mm
1.016	2.00 db/mm
1.168	4.00 db/mm

This large difference in the rate of field decrease for the two fence guides needs further consideration.

Exponential Decay of the Field

The exponential decay of vertical component of the electric field normal to the dielectric-plane was measured at various

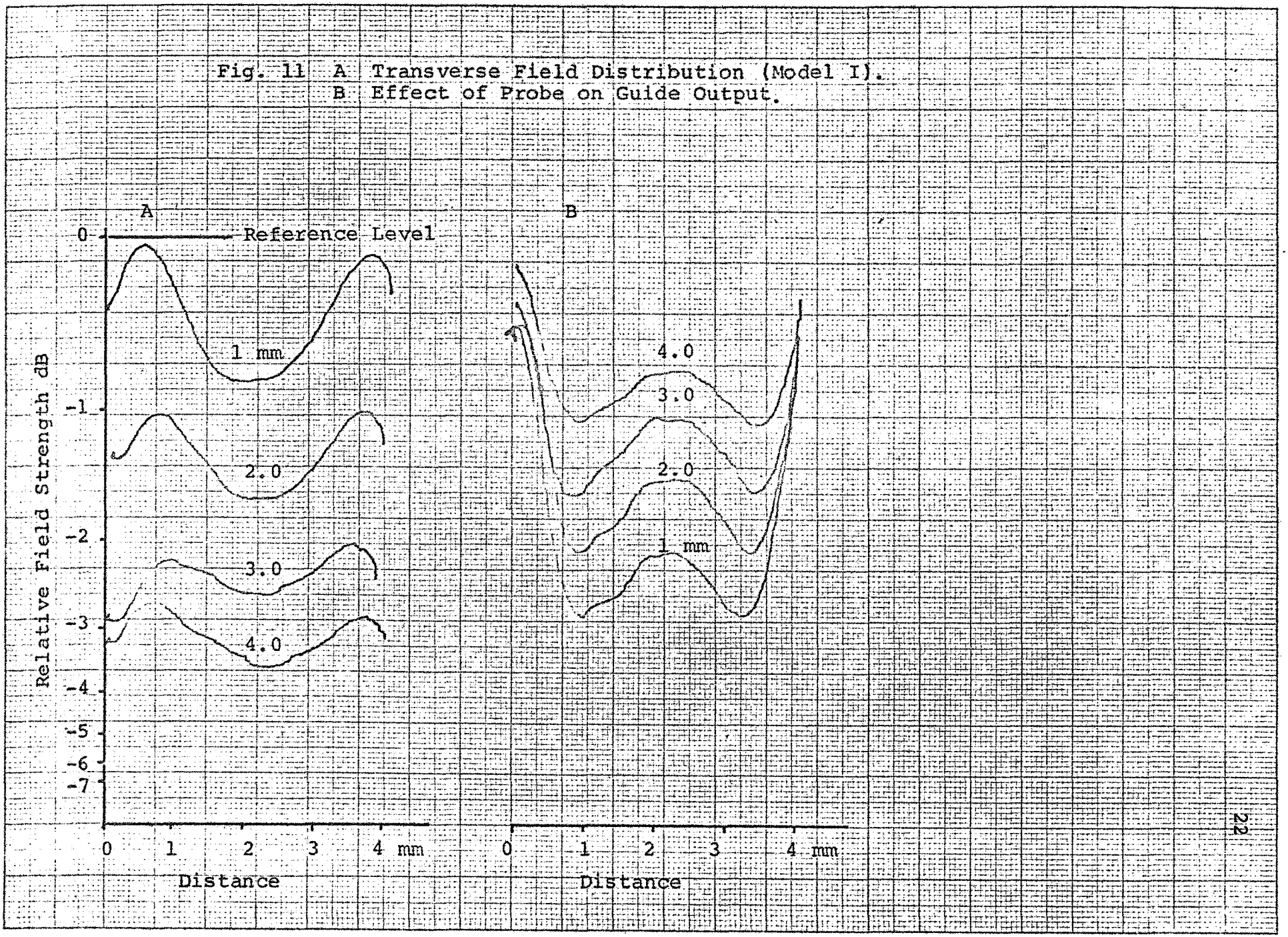

Fig. 11 A Transverse Field Distribution (Model I).
B Effect of Probe on Guide Output.

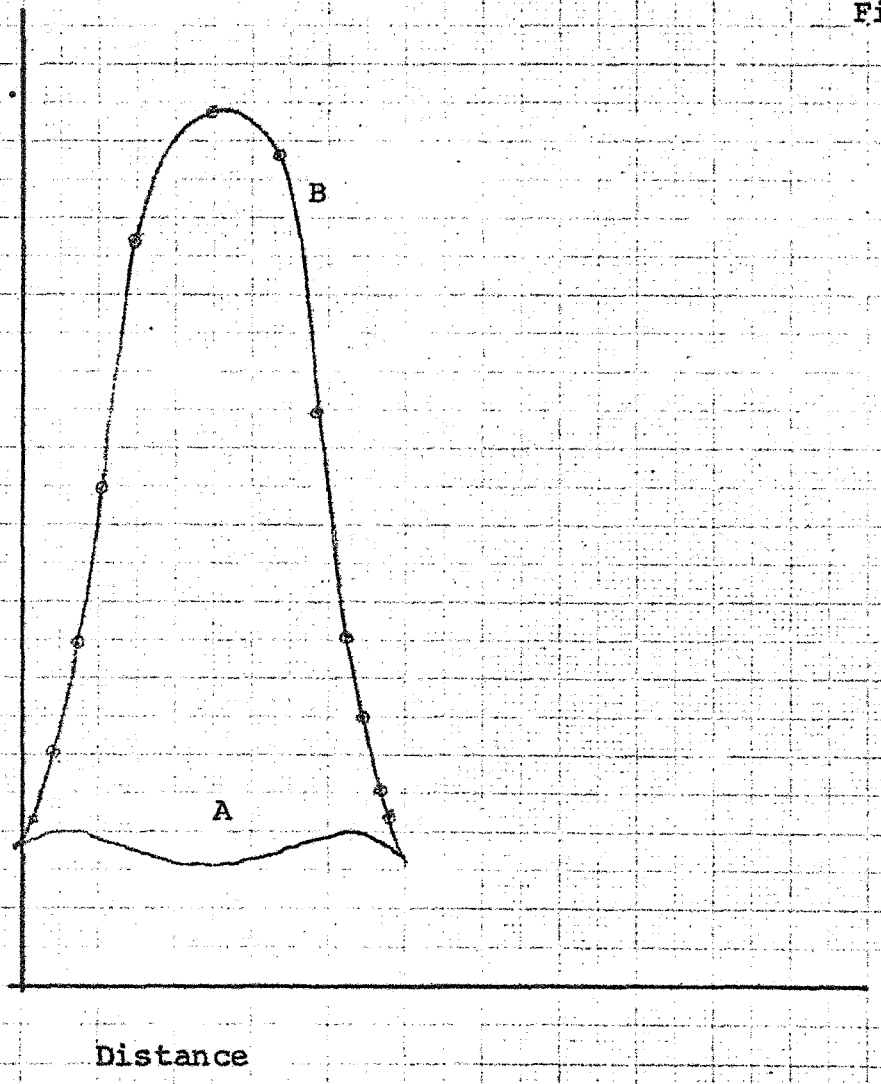

Fig. 12 Transverse Field Distribution (Model I).
A Uncompensated.
B Compensated.

Fig. 13 Transverse Field Distribution above the Fence Guide
Model II, F = 35.04 GHz, above Second Maximum.

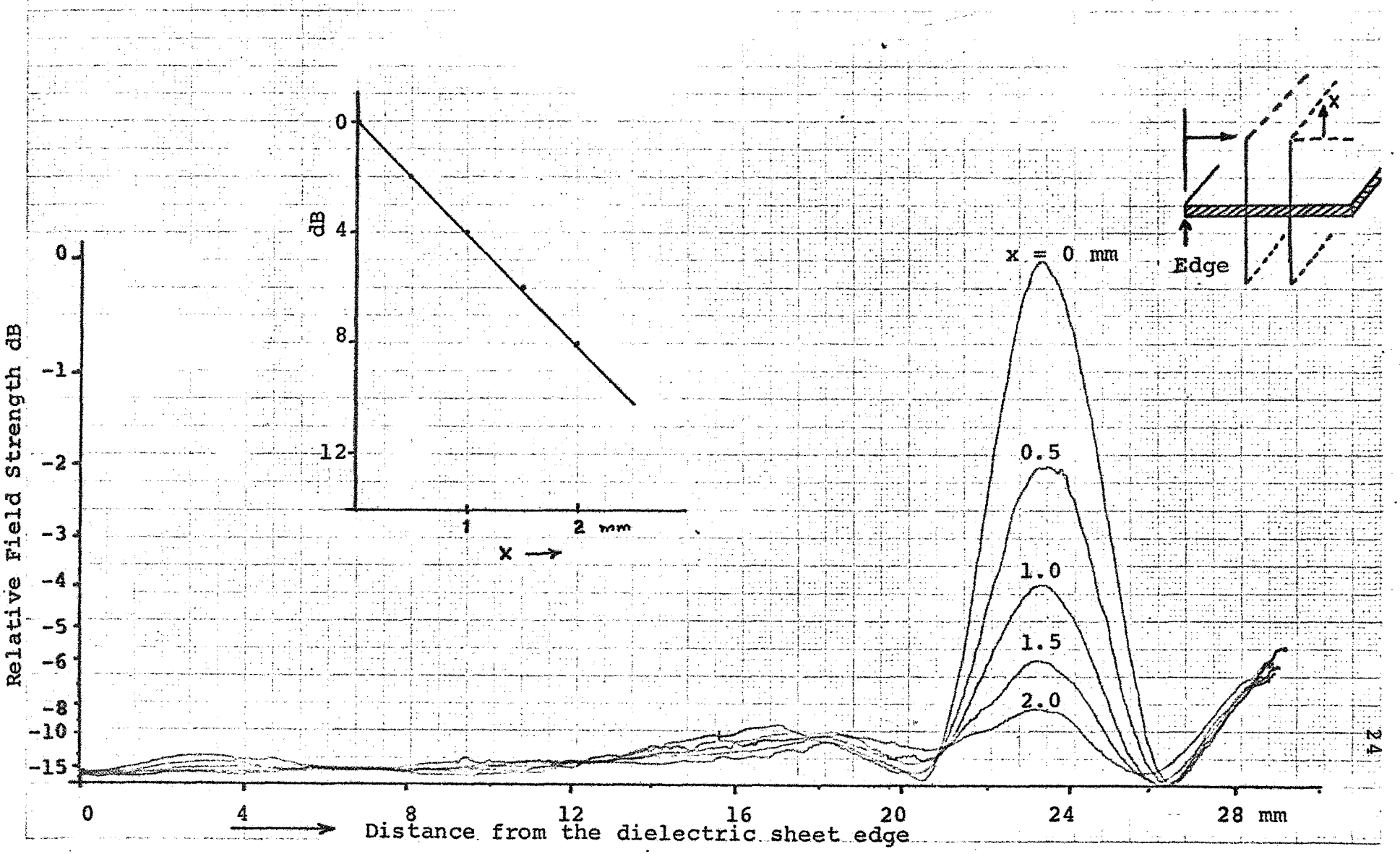

locations with the fence guides short circuited. The curves at the third maximum at the center and near the fence are Fig. 14 to Fig. 16. Both, for compensated and uncompensated cases, the curves were then plotted on a linear scale. The slope of the curves giving the decay factor α_x for the field on the fence guides are tabulated below:

Table III

	α_x in db/mm in third maximum (center)			
	Fence guide wire spacing 1.168 mm		Fence guide wire spacing 1.016 mm	
	Lower region	Upper reg.	Lower reg.	Upper reg.
Uncompensated	1.66	3.70	1.20	2.95
Compensated	—	—	2.30	3.15
	α_x in db/mm near fence in the third maximum			
Uncompensated	1.90	2.40	1.00	2.70
Compensated	2.58	2.58	1.45	2.25

Two different values of α_x were observed, one near the dielectric sheet and up to a height of about 6 mm (lower part) and another value much larger in the upper region extending to the edge of the fence. The compensated values are higher than uncompensated except for one case. Almost in all the measurements the field decays faster in the fence guide with widely spaced wires.

From the measurements of the fence guides the effects of the

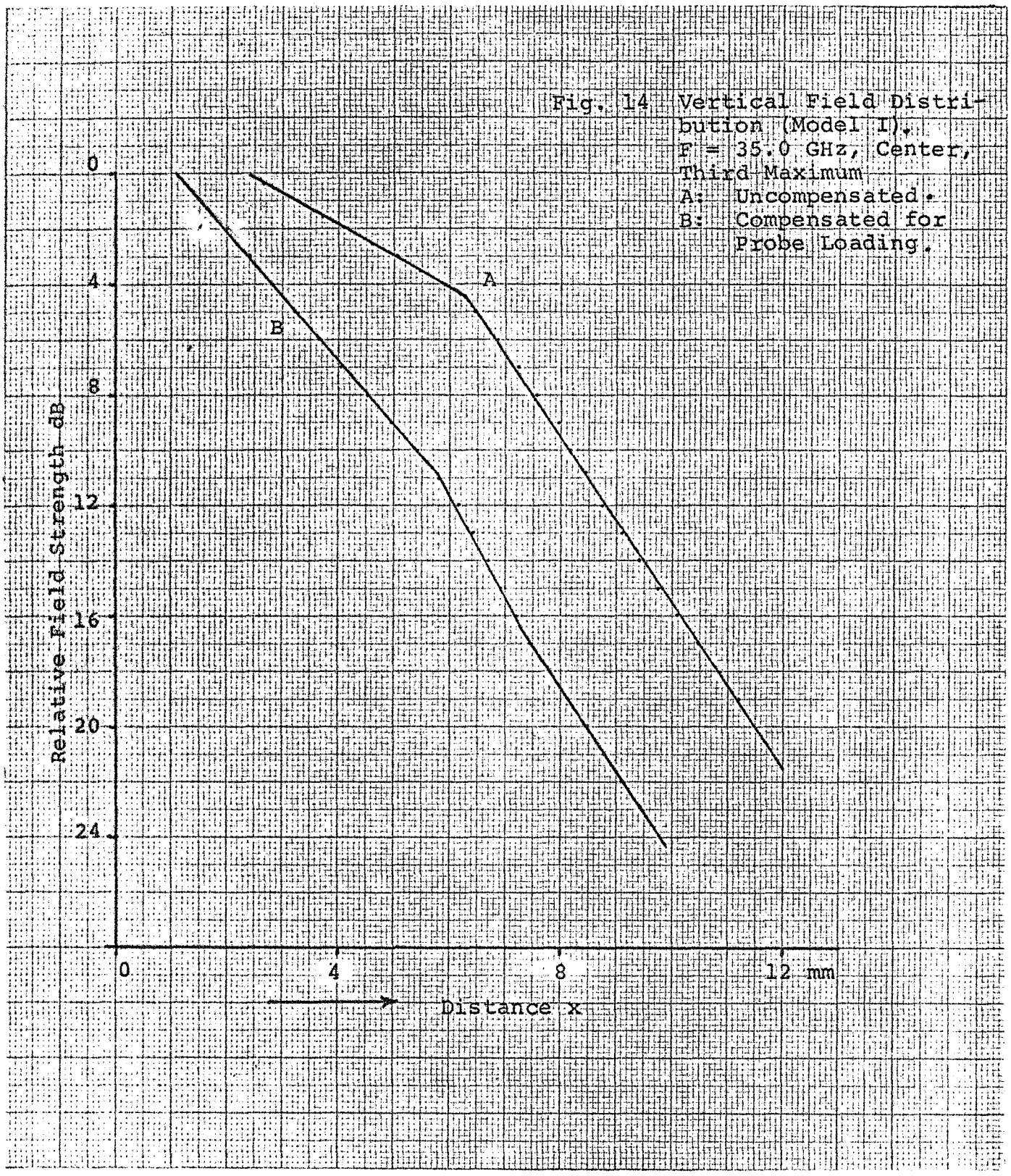

Fig. 14 Vertical Field Distribution (Model I).
F = 35.0 GHz, Center, Third Maximum
A: Uncompensated.
B: Compensated for Probe Loading.

Fig. 15 Vertical Field Distribution (Model II)
(At various longitudinal positions)
1: At maxima
2: At .25 mm away from max.
3: At .50 mm away from max.
4: At .75 mm away from max.

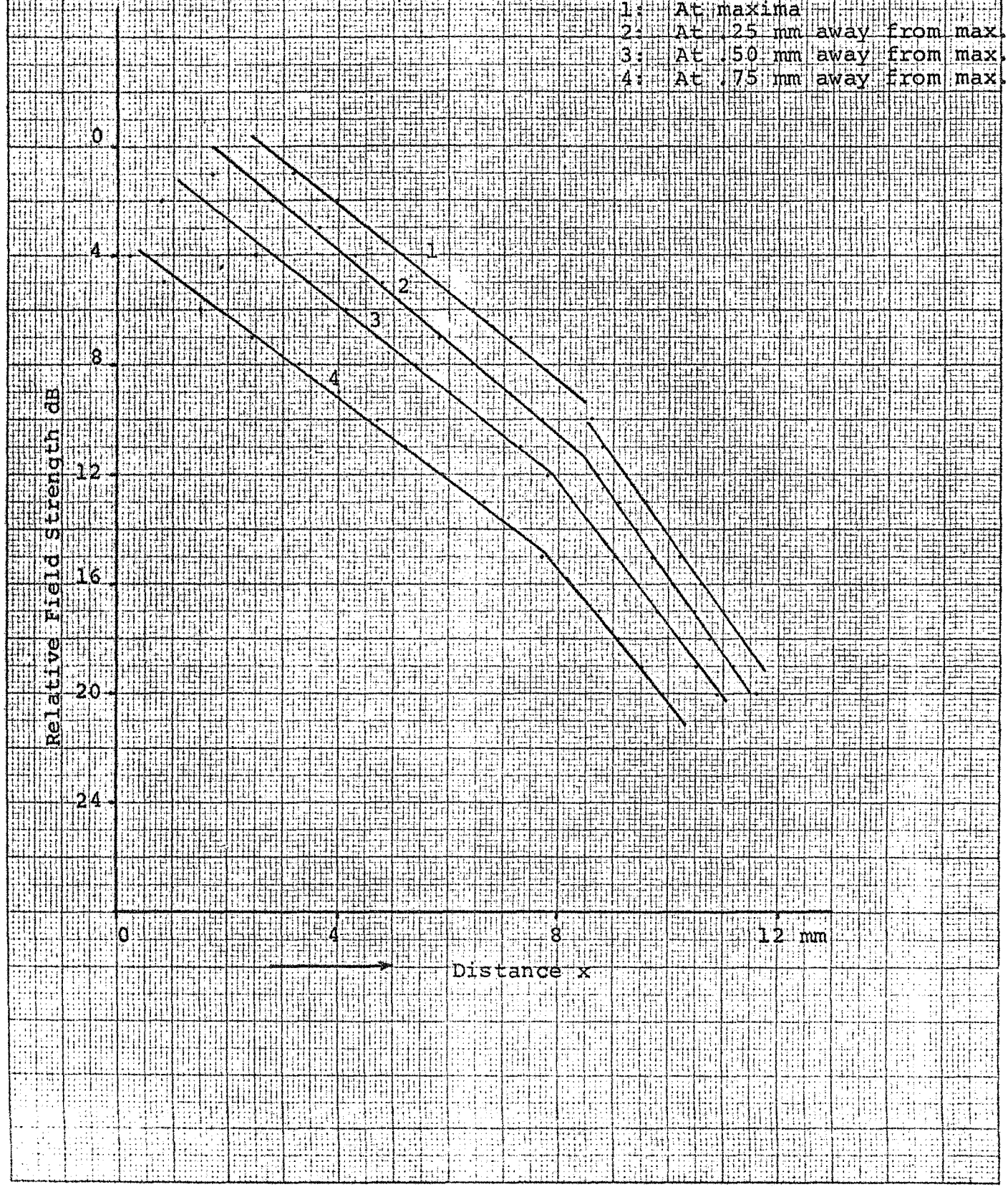

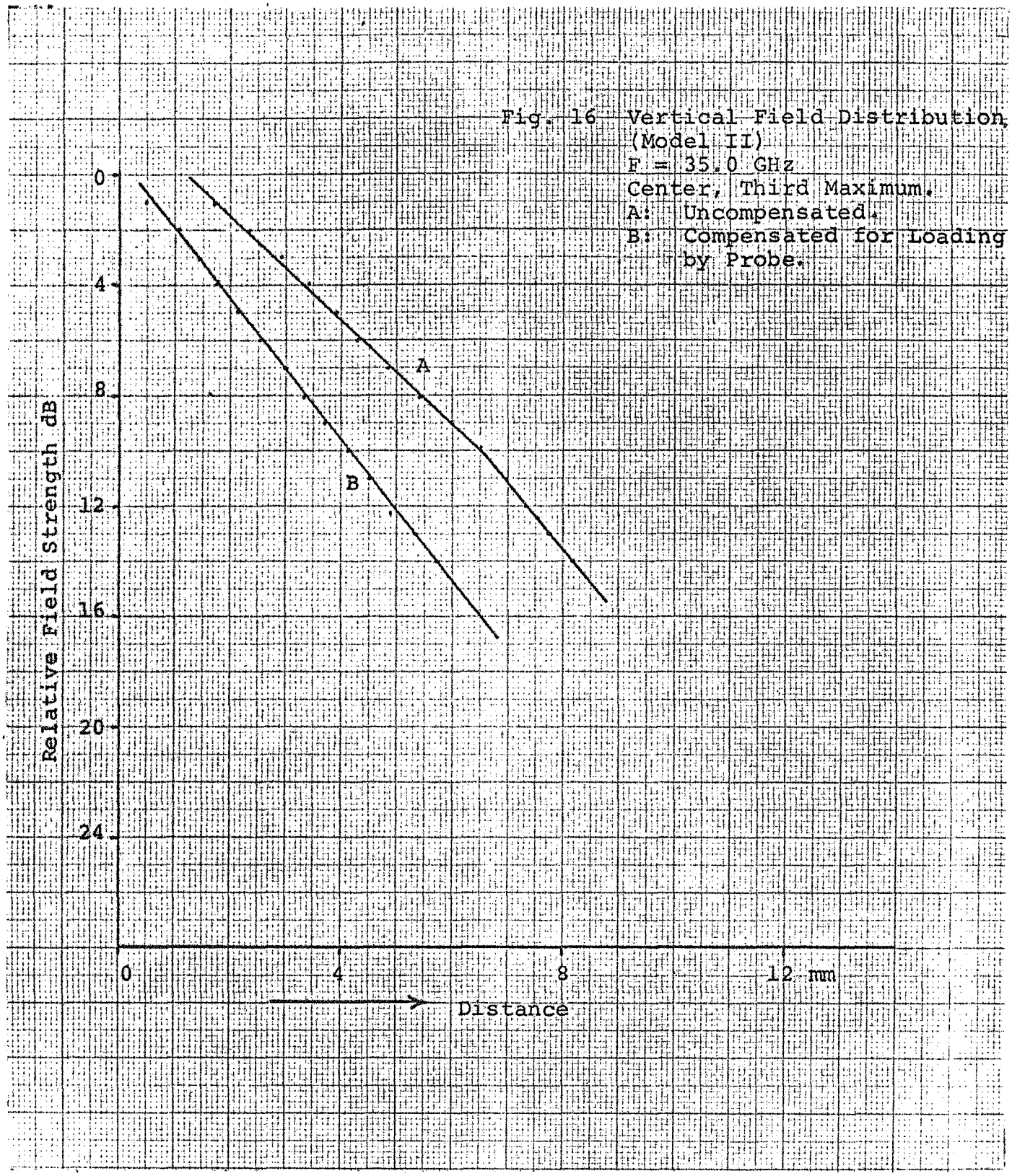

Fig. 16 Vertical Field Distribution (Model II)
F = 35.0 GHz
Center, Third Maximum.
A: Uncompensated.
B: Compensated for Loading by Probe.

changes in the grid spacing are inconclusive. The mechanical tolerances and measurement accuracy together tend to mask the effects of small changes in grid spacings. Further investigations are in progress.

Appendix I

Loading Effects Due to the Probe

In field measurements using probes, it is essential to keep distortions of the fields by the probes at a minimum. In fence guide measurements a capacitive monopole with compensation is being used as a probe. The assembly has a maximum diameter of 1.70 mm and a coax-cable of 0.82 mm size is used. The relative size of the probe to the wavelength is shown in Fig. 17. As can be seen, the size of the probe is no longer small and there was considerable loading of the field due to the probe.

Through a coupling hole with coupling in the order of -20 db, the output power was continuously monitored and variations of as much as 10-12 db were observed. The plots of this change in power level (called loading curves) are included for various field measurements. A typical plot is Fig. 3 . By changing the input power level by a variable attenuator, the output power level was then kept constant for the compensation of the loading effect. Compensated plots are shown in Fig. 12.

The following preliminary observations can be made from the various loading curves:

(1) The amount of loading depends on the intensity of the field, the higher the intensity, the larger the loading and vice versa.

(2) Considerable distortion in the field distribution results due to loading. In some cases, double peaks could be observed which were reduced or completely eliminated after compensation for loading.

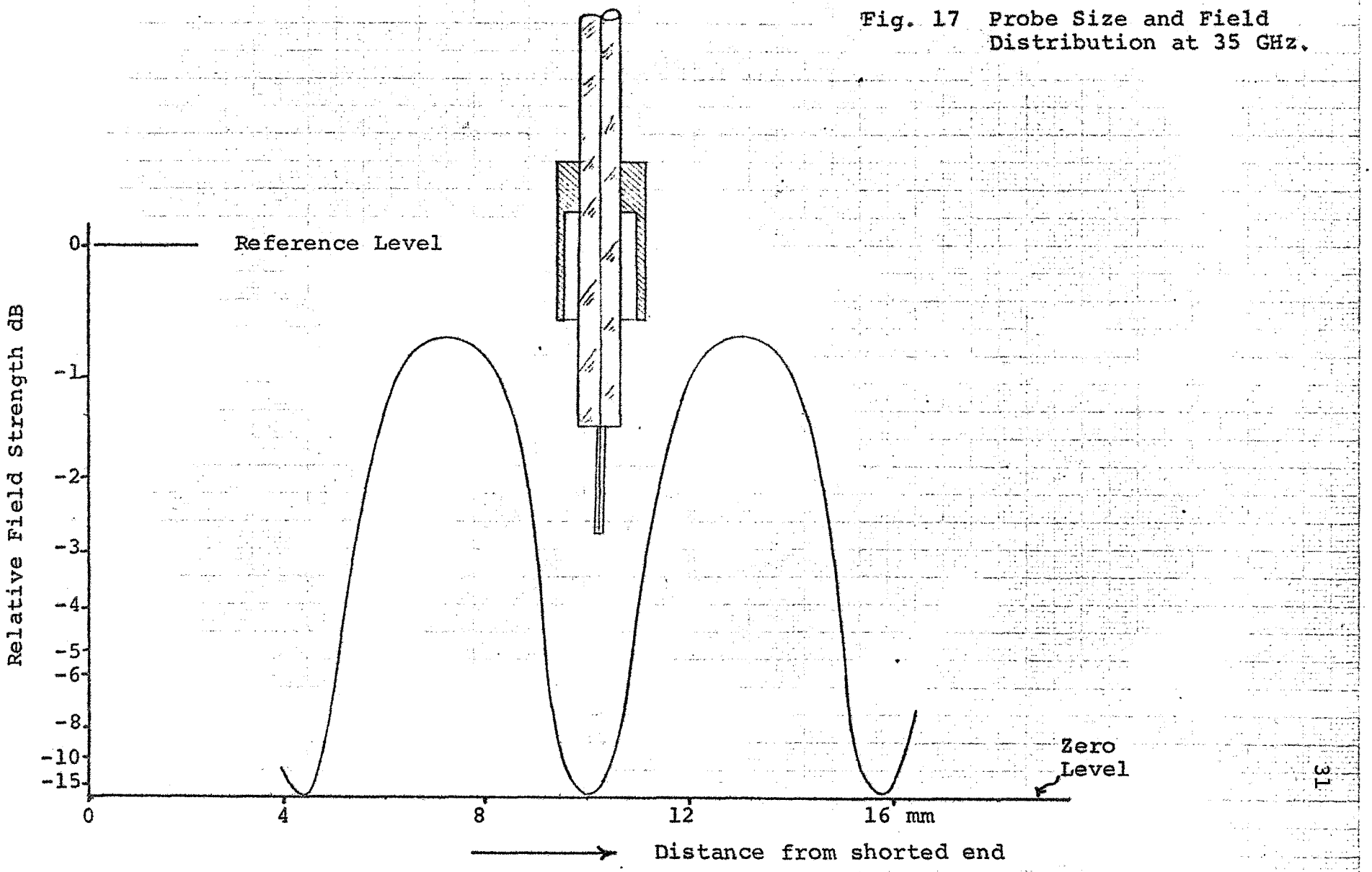

Fig. 17 Probe Size and Field Distribution at 35 GHz.

(3) The measured field due to loading is lower by the amount of the loading.

It is planned to investigate the effect of probe size on loading and on the methods of compensating for the loading effects.

Appendix II

A study of the capacitive monopole was made to see the effects of compensation and change in length on the signal picked up by the probe. Longitudinal field distributions were observed and evaluated in the fence guide with:

(1) Quarter wave monopole - 2.1 mm long

(2) $\lambda/8$ mm monopole

(3) 0.5 mm monopole

(4) Compensated quarter wave monopole

The following observations can be made from the plots:

(1) The form of distribution is not effected by the type of probe used and

(2) The compensated $\lambda/4$ probe has the strongest signal output.

The quarter wave monopole with compensation seems to be the best among the tested probes and is used for the measurements.

EXPERIMENTAL DETERMINATION OF THE Q-VALUES OF TWO FENCE GUIDE RESONATORS

Abstract

Two resonators using fence guides with different spacings of the posts of the wire grids were constructed and preliminary Q-measurements were carried out. The fence guide resonators were then loaded by inserting 1/32" thick Rexolite strips on top of the dielectric slabs between the wire grids. Further loading was obtained by adding a second strip of Rexolite. Increased Q-values were obtained by the loading. The measured Q-values were then used for the computation of the attenuation of the fence guide.

EXPERIMENTAL DETERMINATION OF THE Q-VALUES OF TWO FENCE GUIDE RESONATORS

Introduction

One of the conventional methods for the measurement of the attenuation of a waveguide system involves the measurement of the longitudinal field distribution. From the envelope of the distribution, the attenuation of the waveguide can be determined. This technique was applied to determine the attenuation of a fence guide and a preliminary figure for attenuation was quoted in the progress report NGL 34-002-047 dated June 15, 1970. The field probing technique, however, is affected by field distortions and probe-loading effects and large errors might result. This is particularly true when the device to be evaluated has low attenuation. A more accurate method is based on the measurement of the Q-factor of a resonator formed by a section of the guide under investigation. The method involves the measurement of the difference of the half power frequencies of the output signal and insertion loss of the transmission-type resonator.

Two cavity resonators, each 175 mm long, were built by using fence guides with different spacings of the wires of the wire grid side walls, s_w = 1.168 mm and s_w = 1.016 mm. To couple the energy in and out of the resonators, copper plates with a single circular hole were used on both ends. The holes were positioned symmetrically to the dielectric sheet of the fence guide. The copper plates also represent the end walls of the two connecting rectangular input and output waveguides.

Q-Value Measurements

Measurements were made using the setup and technique outlined in Progress Report NGR 34-002-047/S2 of February 15, 1969. The values of loaded Q were determined using the well known relationship

$$Q_L = \frac{f_o}{\Delta f} ,$$

where

f_o = resonant frequency of the resonator,

Δf = 3 dB - bandwidth of the resonator.

The Q-values of the two proto-type fence guide resonators were measured and compared.

Effects of increasing the thickness of the dielectric slab within the fence guide on the loaded Q of the fence guide resonators was also studied. The resonators were loaded with 1/32" thick Rexolite (ε_r = 2.53) strips over their full length. The measured values of the loaded Q and of the insertion loss of the two resonators under various conditions of loading and for various resonant frequencies are tabulated in Table 1 and Table 2.

Evaluation of the Measurements

The following observations about the behavior of the resonators can be made:

(1) The fence guide resonator with larger wire spacing (s_w = 1.168 mm) has slightly higher resonant frequencies.

(2) The insertion losses for the two resonators under similar loading conditions are approximately equal.

(3) The fence guide resonator with narrow wire spacing

(s_w = 1.016 mm) has somewhat higher loaded Q-values in the region of higher frequencies.

(4) With increasing loading, the number of wave modes is larger for both resonators.

(5) Higher values of loaded Q are measured when the resonators are loaded with a single 1/32" Rexolite strip. The loaded Q-values decrease again when a second 1/32" Rexolite strip was added.

(6) The resonant frequency is slightly lower at loading with Rexolite strips.

Fence Guide Attenuation

One of the basic informations that can be obtained from Q-measurements is the loss property of the structure. Tables 1 and 2 list the values of loaded Q and insertion loss, from which the unloaded Q of the fence guide resonators can be computed. The insertion loss is in the order of 30 dB or greater and the unloaded Q is about 104% or less of the loaded Q[3]. The attenuation was computed using the relationship

$$\alpha \simeq \frac{k_o^2}{2k_z Q} ,$$

where $k_o = \frac{2\pi}{\lambda_o}$; λ_o being free space wavelength,

$k_z = \frac{2\pi}{\lambda_g}$; λ_g being guide wavelength,

Q = Unloaded Q of the resonator.

The data of Fig. 10, guide wavelength for fence guides[4] are used to compute k_z. The values of attenuation α in dB/mm are given for the two fence guides at various frequencies in the

34.0 - 37.0 GHz range in Tables 3 and 4. The attenuation of the fence guides loaded with one and two strips of 1/32" thick Rexolite ($\varepsilon_r = 2.53$) are also included in the tables. The computation for the loaded guides are based upon the guide wavelength graphs[4] for the unloaded fence guides.

Disregarding some small changes due to mechanical tolerances, the two fence guides differed mainly in the fence post spacing. The attenuation α, for the two fence guides as given in Tables 3 and 4 suggest that a smaller spacing between the fence posts results in a somewhat reduced attenuation. The loading with one Rexolite strip results in a significant reduction of the fence guide losses. Further loading, however, increases the attenuation again. This behavior suggests that there is an optimum loading for minimum attenuation. Further studies are planned to study the effects of loading.

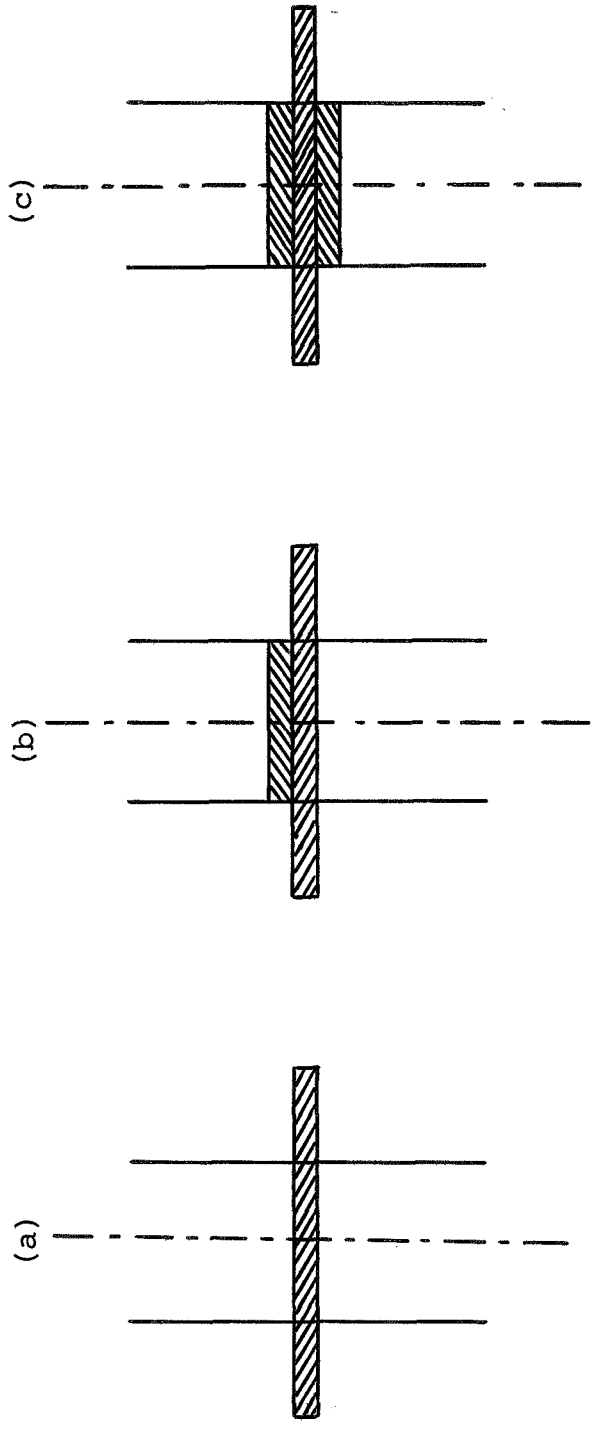

Fig. 1 Dielectric slab configuration of fence guides under investigation.

(a) Single-slab guide.
(b),(c) Dielectric-loaded guides.

Table 1

Resonator with wire spacing s_w = 1.016 mm for three dielectric-slab configurations (Fig. 1).

(a) Unloaded.
(b) Loaded, single strip.
(c) Loaded, double strip.

	Resonant Freq. f_o (GHz)	Insertion Loss (dB)	Loaded Q
(a)	34.290	46.60	496.09
	34.861	42.32	701.15
	36.037	39.65	796.58
	36.615	31.70	1704.63
(b)	34.260	33.70	1659.89
	34.783	35.22	1555.57
	35.318	33.05	1440.38
	35.850	36.80	1413.65
	36.374	23.30	2020.79
	36.615	40.75	2205.73
(c)	34.102	39.05	995.97
	34.574	41.90	842.44
	35.054	38.10	900.65
	35.528	38.00	795.87
	36.006	37.42	835.00
	36.374	37.65	1959.81
	36.615	38.85	1977.03

Table 2

Resonator with fence spacing s_w = 1.168 mm for three dielectric-slab configurations (Fig. 1).

(a) Unloaded.
(b) Loaded, single strip.
(c) Loaded, double strip.

	Resonant Freq. f_o (GHz)	Insertion Loss (dB)	Loaded Q
(a)	34.294	45.12	689.73
	34.875	41.52	767.48
	36.046	41.77	705.66
	36.635	28.20	1554.97
(b)	34.301	33.05	1337.78
	34.826	32.15	1136.61
	35.357	29.75	997.65
	36.381	30.00	1629.95
	36.633	37.35	1999.59
(c)	34.335	36.02	1126.49
	34.819	34.80	920.16
	35.311	32.50	1201.05
	35.783	36.30	1378.39
	36.381	36.15	1169.04
	36.633	36.00	2180.56

Table 3

Fence guide with spacing s_w = 1.016 mm for three dielectric-slab configurations (Fig. 1).

(a) Unloaded.
(b) Loaded, single strip.
(c) Loaded, double strip.

	Frequency GHz	Guide wavelength (mm)	Unloaded Q	Attenuation α(dB/mm).
(a)	34.290	11.603	498.57	0.00829
	34.861	11.265	706.76	0.00587
	36.037	10.610	805.34	0.00518
	36.615	10.320	1750.65	0.00239
(b)	34.260	11.620	1694.75	0.00244
	34.783	11.305	1583.57	0.00262
	35.318	11.005	1473.51	0.00282
	35.850	10.710	1434.85	0.00291
	36.374	10.440	2164.27	0.00193
	36.615	10.320	2225.58	0.00188
(c)	34.102	11.730	1006.93	0.00411
	34.574	11.430	849.18	0.00488
	35.054	11.155	911.91	0.00456
	35.528	10.890	805.82	0.00517
	36.006	10.630	846.69	0.00493
	36.374	10.440	1985.29	0.00211
	36.615	10.320	1998.78	0.00210

Table 4

Fence guide with spacing s_w = 1.168 mm for three dielectric-slab configurations (Fig. 1).

(a) Unloaded.
(b) Loaded, single strip.
(c) Loaded, double strip.

	Frequency GHz	Guide wavelength (mm)	Unloaded Q	Attenuation α (dB/mm)
(a)	34.294	11.68	693.87	0.00600
	34.875	11.32	773.62	0.00539
	36.046	10.605	711.30	0.00587
	36.635	10.270	1617.17	0.00258
(b)	34.301	11.67	1368.55	0.00304
	34.826	11.34	1166.16	0.00358
	35.357	11.03	1030.54	0.00406
	36.381	10.41	1683.74	0.00248
	36.633	10.27	2027.58	0.00206
(c)	34.335	11.645	1144.51	0.00364
	34.819	11.345	936.72	0.00445
	35.311	11.055	1230.47	0.00339
	35.783	10.765	1400.44	0.00298
	36.381	10.408	1187.74	0.00352
	36.633	10.270	2215.45	0.00189

References

1. Progress Report, Grant NGL 34-002-047, N. C. State University, June 15, 1970.

2. Progress Report, Grant NGR 34-002-047/S2, N. C. State University, February 15, 1969.

3. Montgomery, et al., "Principles of Microwave Circuits" pp. 237-239, Boston Technical Publications, 1964.

4. Dr. F. J. Tischer, K. K. Agarwal, "Comparative Study of Fence Guide Fields", same progress report.

DIELECTRICALLY LOADED PARALLEL-WALL GUIDE

Abstract

The characteristics of a parallel-wall waveguide loaded with dielectrics of three different geometries are experimentally investigated. Preliminary results of measurements of the longitudinal and transverse field distributions and their evaluation are presented. The field decrease towards the guide opening, the guide wavelength, and the Q-value of the waveguide are computed. The following dielectric structures were considered:

(a) H-guide configuration - the dielectric strip perpendicular to the side walls.

(b) Dielectric strip parallel to the side walls.

(c) Dielectric rod.

Description of the Guide

The waveguide consists of two copper side walls and the dielectric structure in the center. Fig. 1a, 1b, and 1c show the three configurations. In the case of the H-guide, the dielectric strip is placed in the center of the guide by attaching it to the sidewalls with double-coated adhesive tape. The dielectrics for the other two guides are supported at each end on a small piece of polystrene foam attached to the end walls of the guides.

The measurements are carried out in a shorted section of the guide with one of the dielectric structures after the other. The detailed composition of the end structure is shown in Fig. 1d. The resonator end-wall with a circular coupling hole in the center and the end-plate are fastened by screws to the end surfaces of the sidewalls. Energy is fed from an open-ended waveguide into a rectangular hole in the end-plate and is coupled through the circular hole into the waveguide.

Measurement Setup

The procedure and the equipment for the field distribution and Q-measurements were described in two previous reports.[1,2] The distribution of the vertical component of the electric field intensity in the longitudinal and transverse directions were obtained using a compensated capacitive probe. The probe was also described in an earlier progress report.[2]

Results of Field Measurement

Longitudinal field distributions at several locations in the transverse plane of each of the waveguides were obtained on

an x-y plotter. The guide wavelengths can then be computed from such graphs. Two sample field profiles are shown in Fig. 2 and Fig. 3.

In order to find the exponential field decrease, the actual field variation in the x-direction was measured at various longitudinal and transverse positions. The graphs were then replotted on linear scales. The slope of the resulting linear graph yields the field decrease in dB per unit length.

For each waveguide the field decrease was measured at various points along the guide, and an average determined. Figures 4a through 4e show the averages of the vertical field decreases on a linearized dB-scale. Each graph shows a large number of measurement points and the linear average for one of the guides. Table I gives a summary of the results of the evaluation of these measurements.

Result of Q-Measurements

Tables II through IV give the Q-values and the associated values of insertion loss measured for the type of waveguides indicated at the top of each table. The listed values of Q are those for loaded sections of the guide. The unloaded values can be computed by the use of an equation shown in Progress Report of February 15, 1969, page 25.

In the case of the H-guide configuration having a 0.508 mm thick lucalox center dielectric, the Q-values of a few modes were re-measured with both openings of the guide covered with absorbing material. It was observed that the maximum change in Q-value for the modes measured was about 15%.

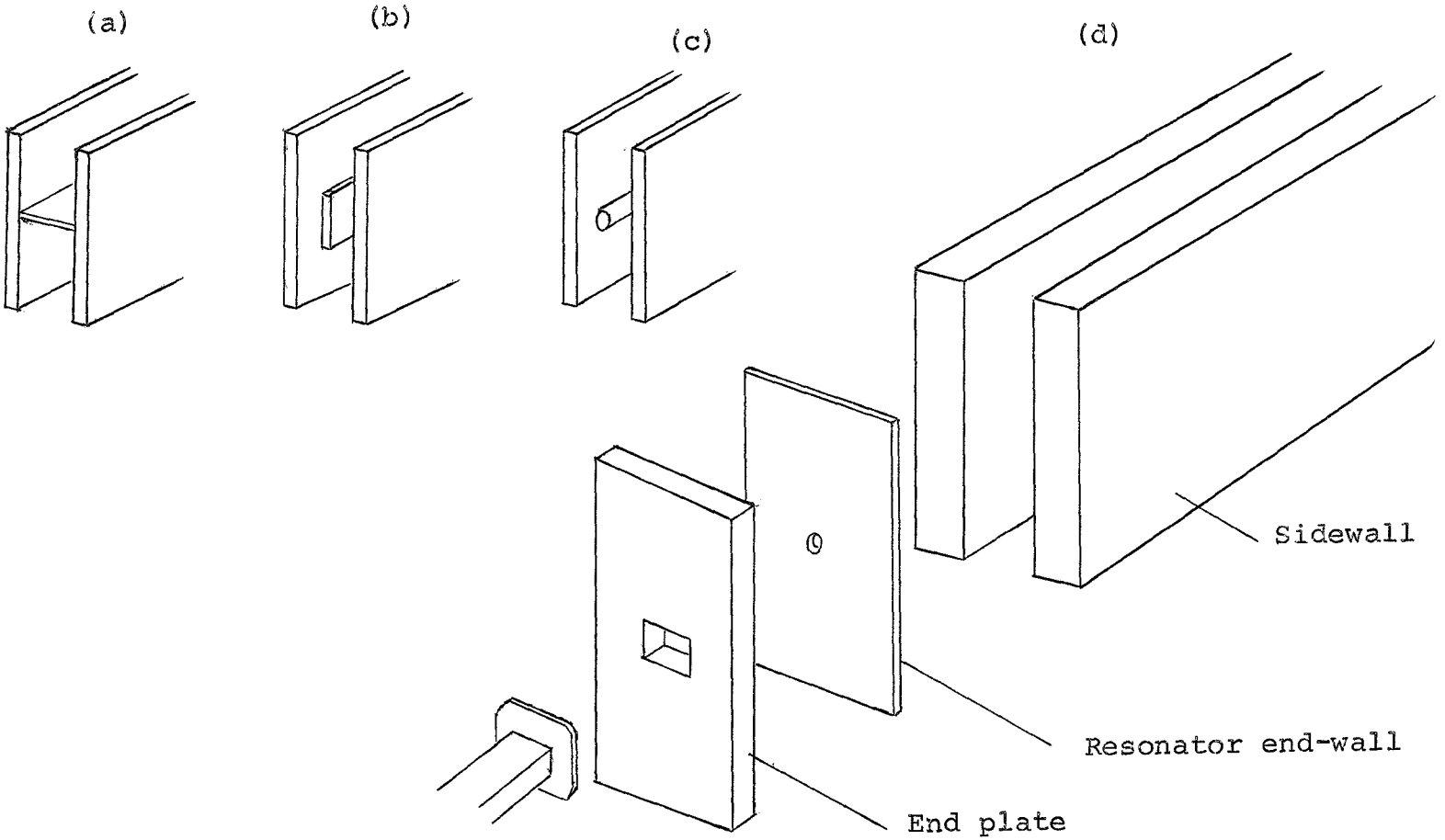

Fig. 1 Parallel-wall waveguide with various dielectric-loading configurations.

(a) Dielectric strip right angle to sidewalls - H-guide geometry.
(b) Dielectric strip parallel to sidewalls .
(c) Dielectric rod .
(d) Waveguide construction .

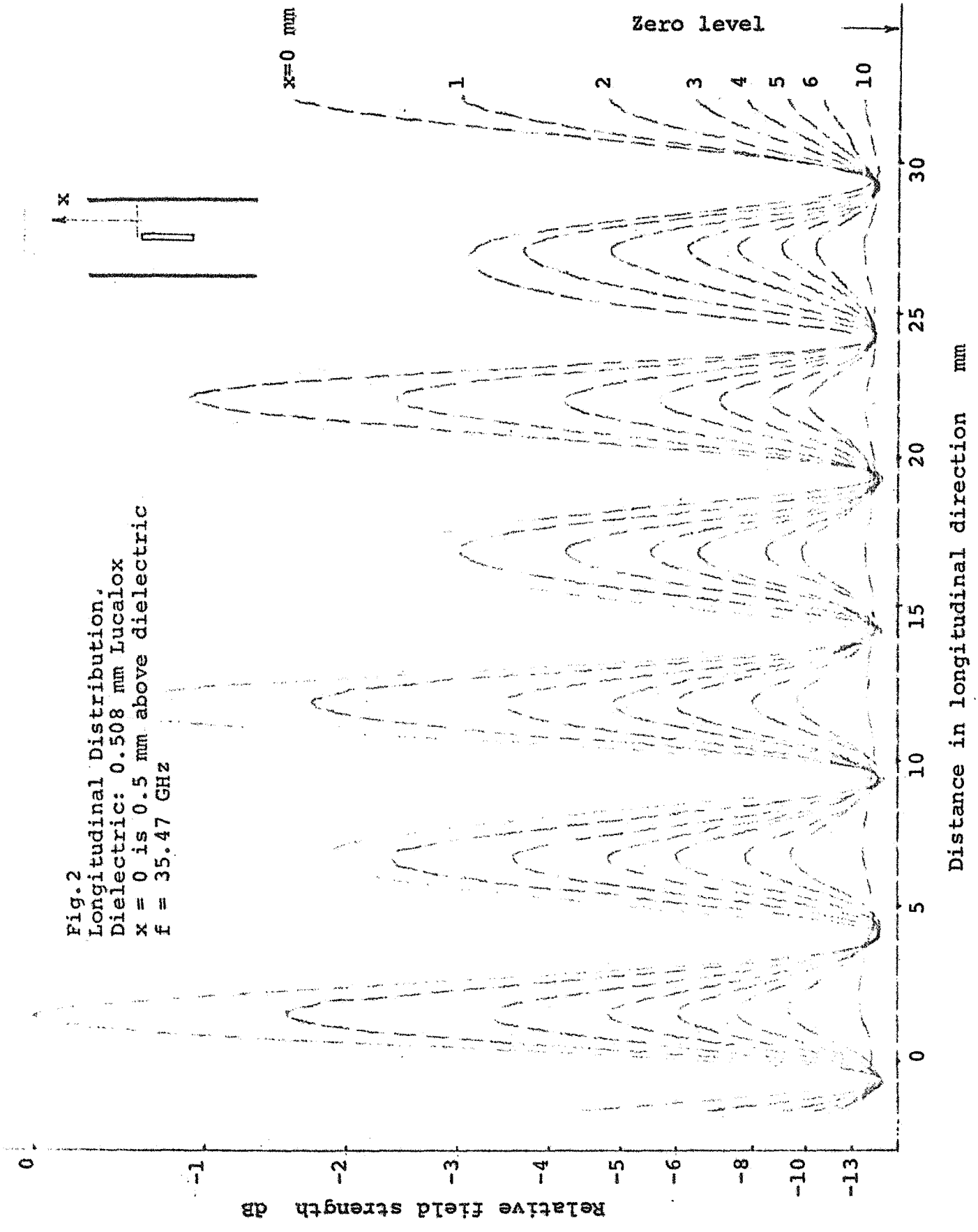

Fig.2
Longitudinal Distribution.
Dielectric: 0.508 mm Lucalox
x = 0 is 0.5 mm above dielectric
f = 35.47 GHz

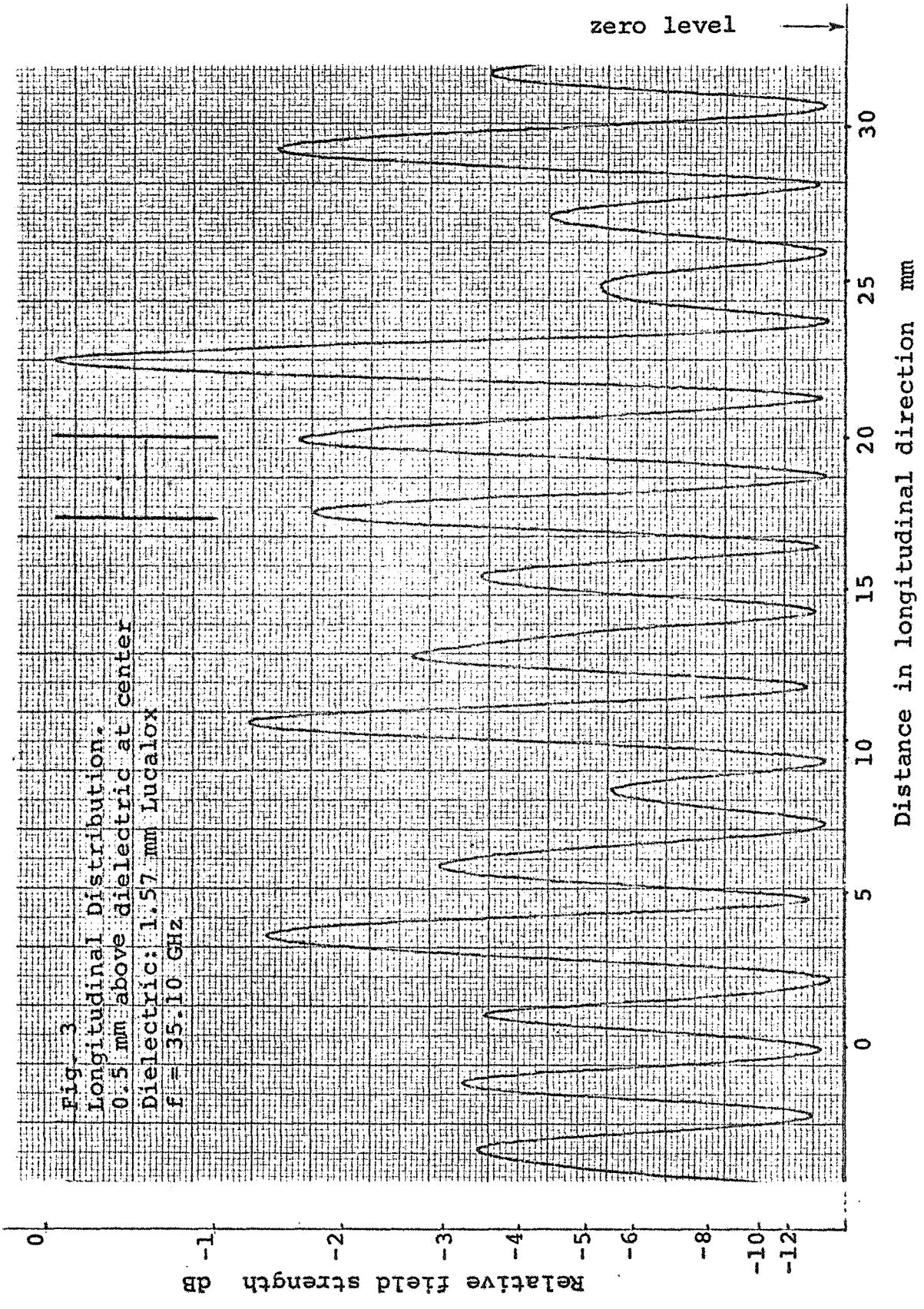

Fig. 3
Longitudinal Distribution.
0.5 mm above dielectric at center
Dielectric: 1.57 mm Lucalox
f = 35.10 GHz

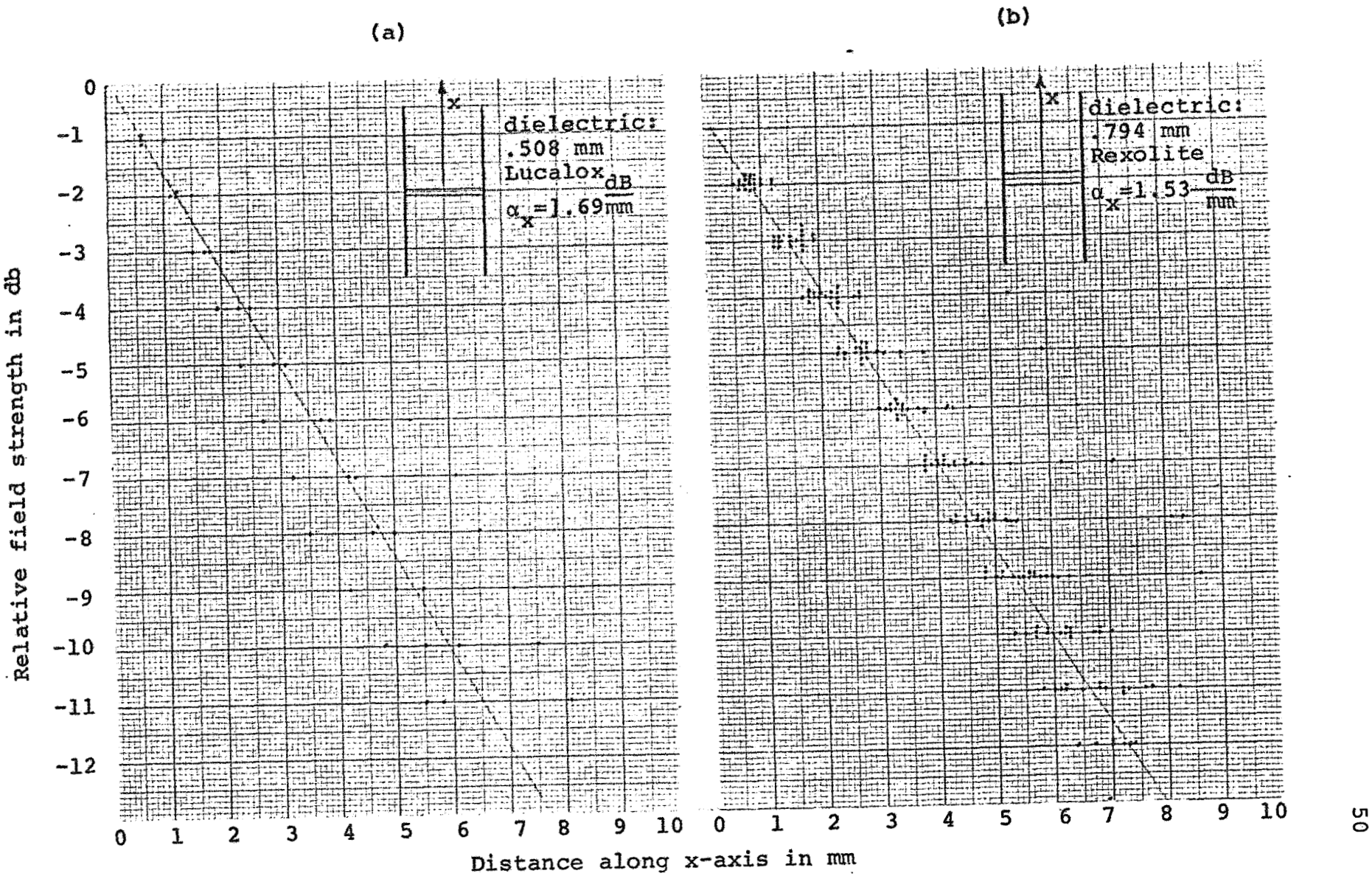

Fig. 4a,b Field decrease in vertical direction.

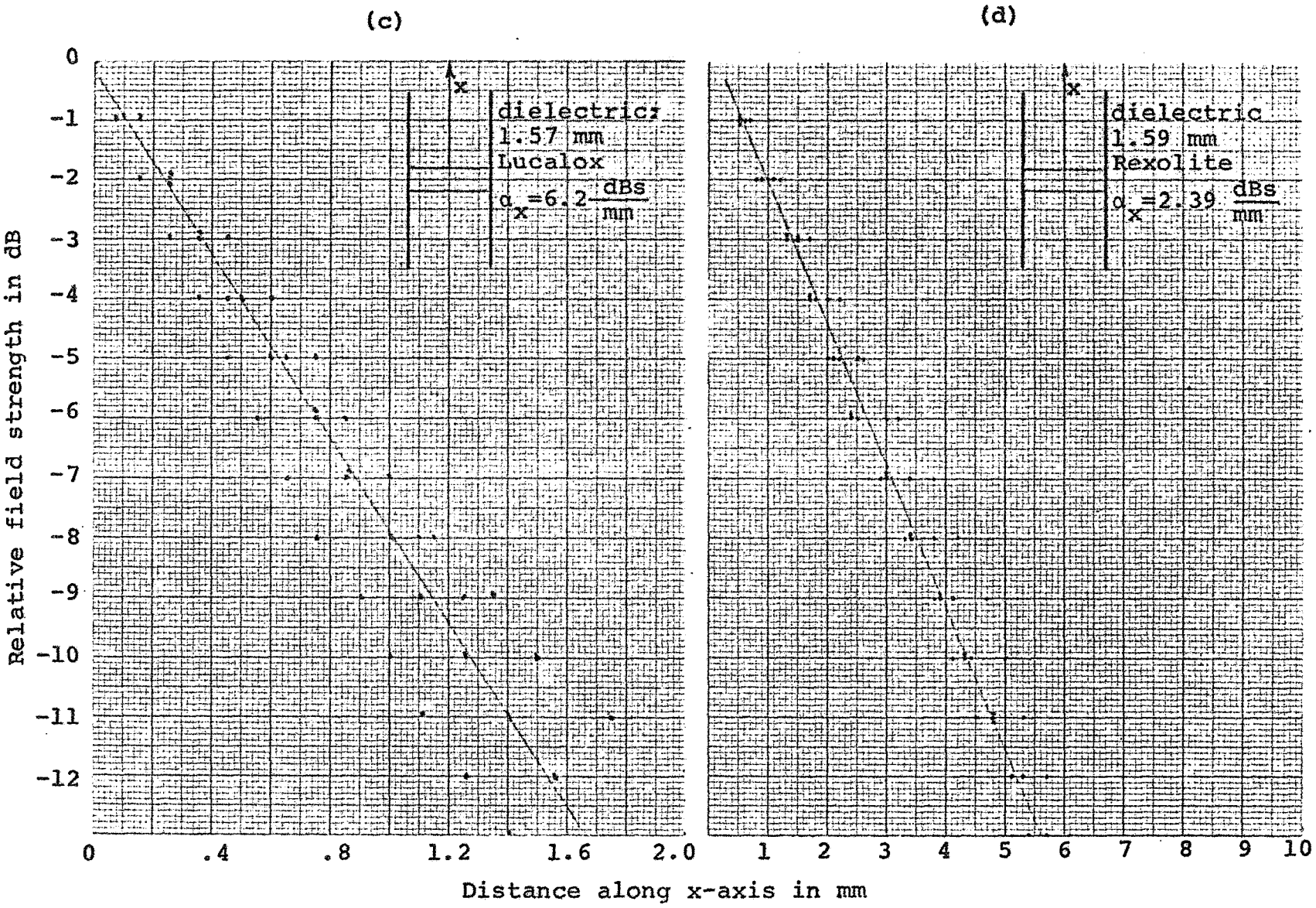

Fig. 4c,d Field decrease in x-direction.

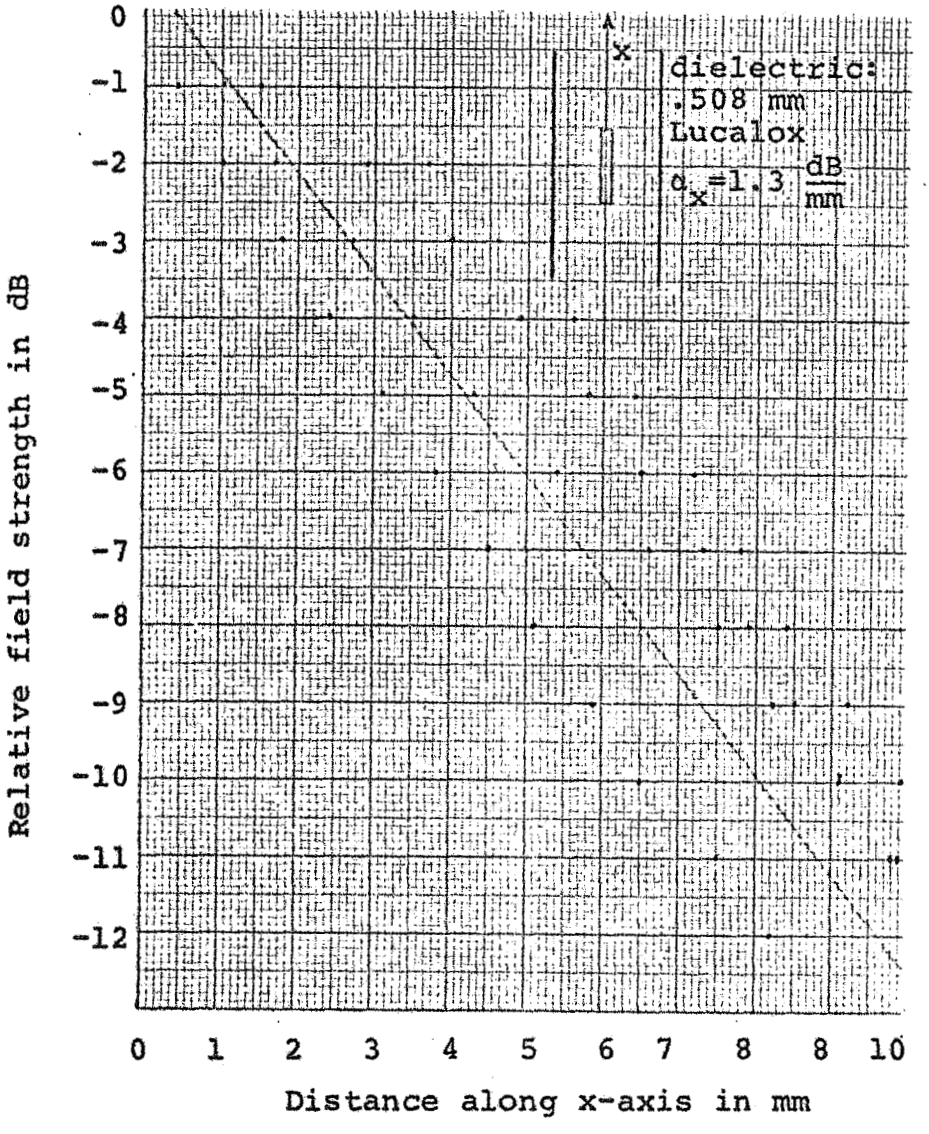

Fig. 4e Field decrease in x-direction.

References

1. R. Packard, F. J. Tischer: Q-value Measurements on Shorted H-guide Test Sections, Progress Report, Grant NGR 34-002-047/S2, pp. 4-27 (February 15, 1969).

2. R. A. Kraft, M. D. Summerlin: Electromagnetic Field Structure About a Fence Guide, Progress Report, Grant NGL 34-002-047, pp. 53-86 (February 15, 1970).

Table I

Waveguide	Dielectric	Dimensions mm	Frequency GHz	α_x [dB/mm]	Guide wavelengths mm
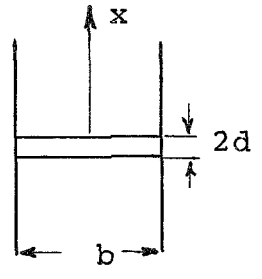	Rexolite	2d = .794 b = 7.1	36.60	1.53	9.55
		2d = 1.59 b = 7.1	35.00	2.39	9.47
	Lucalox*	2d = .508 b = 6.20	35.04	1.69	10.35
		2d = 1.57 b = 6.20	35.1	6.9	4.62
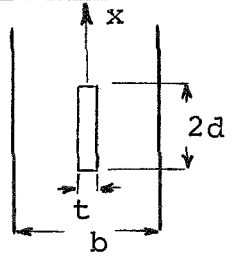	Lucalox	2d = 6.20 b = 7.1 t = .508	35.47	1.30	10.0
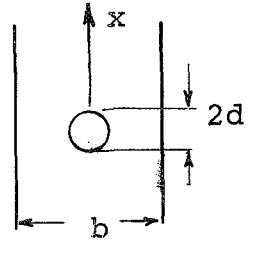	Lucalox	2d = 3.17 b = 7.1	35.37	1.89	9.28

*Ceramic (99.95% AlO_3) by General Electric.

Table II

H-Guide Configuration.

	f GHz	Q-value (Loaded)	Insertion Loss
	35.109	2643	47
0.794 mm	35.674	2526	47.8
Rexolite	36.245	2359	45.9
	34.130	2912	41.6
1.59 mm	34.616	2747	41.5
Rexolite	35.103	3068	40.3
	35.591	2542	41.3
	36.079	2471	39.4
	34.475	5386	42.7
0.508 mm	35.051	5546	39.3
Lucalox	35.576	5232	40.5
	36.107	6182	38.1
	34.416	1781	40
	34.570	2182	36
	34.883	2325	37.6
1.57 mm	35.195	3013	35
Lucalox	35.351	2482	35.3
	35.508	2360	36.7
	35.669	1994	38.5
	35.969	3611	34
	36.134	3041	32.9
	36.295	2592	33.8

Table III

Parallel-Wall Guide with Dielectric Rod.

	f GHz	Q-value (Loaded)	Insertion Loss
3.17 mm			
Diameter	34.848	889	46
Rexolite	35.719	719	44.7
	34.274	3967	47
3.17 mm	34.380	970	45.70
Diameter	35.166	1387	46.4
Lucalox	35.276	1592	45.5

Table IV

Guide with Dielectric Strip Parallel to Walls.

	f GHz	Q-value (Loaded)	Insertion Loss
	34.425	10625	29.9
	34.690	6723	31.8
	34.911	6713	33.5
.508 mm thick	35.218	3412	35.7
Lucalox	35.512	10684	30.2
	35.704	7694	32.4
	35.996	6766	30.4
	36.256	4577	32.3
	36.769	11210	26.3
	34.369	1715	47.
.794 mm thick	34.869	1660	47.
Rexolite	35.372	1524	46.8
	35.875	1627	46.7

EFFECTS OF SURFACE ROUGHNESS AT MILLIMETER WAVES

Abstract

Preliminary results of Q-value measurements for the study of the effects of surface roughness are given. The results indicate that the Q-value of resonators decreases with increasing roughness. Data are given which illustrate the effect.

Introduction

This paper describes a continuation of the study of the effects of surface properties on the surface resistance. In a previous report a technique was discussed for measuring surface roughness by light reflectance. By using this technique and by measuring the Q-values of resonators with varying side wall roughness, it was found that a considerable effect is caused by surface effects. For the two cases considered, the conventional resonator and a closed H-guide resonator, the Q-values decrease with increasing surface roughness.

Description of the Resonator

The resonators have a rectangular form and have removable side walls. A photograph of the resonator with a dielectric strip is shown in Fig. 1. Originally, a regular rectangular resonator was used with six individual walls. This design made the Q-value of the resonator sensitive to the torque exerted on the screws when the resonator was assembled. The design was then changed to keep the upper and lower walls permanently attached to the front and back walls, giving a maximum Q-value, and allowing

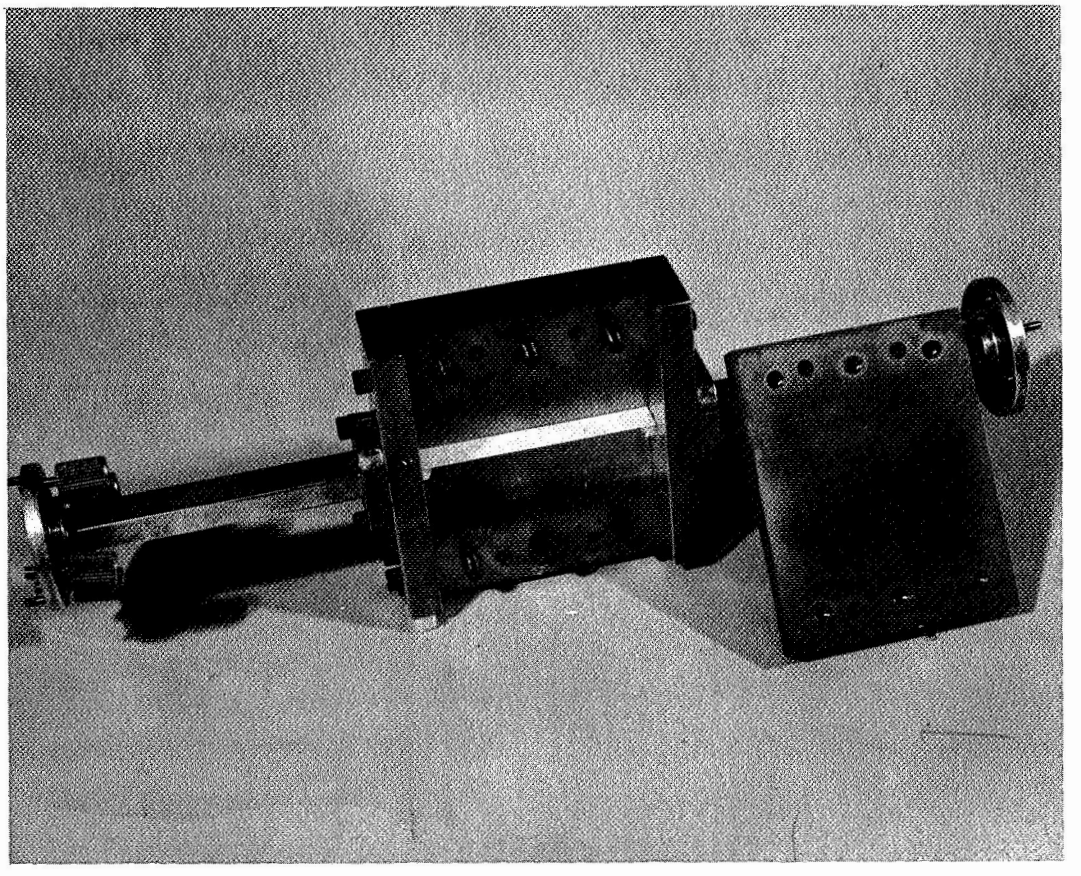

Fig. 1 Closed H-guide resonator with a side wall removed.

the removal of the side walls without disturbing the rest of the setup. With this arrangement, the walls can be removed and ground to have various degrees of surface roughness. To assure that the side walls return to the same position at the replacement, a flat plate is forced against the bottom of the resonator causing the bottom surfaces of the side walls to lie in the same common plane. The pressure of the screws on the side walls is held constant by torquing the screws to fifteen inch pounds at each assembly and subsequent measurement.

Roughness of the Side Walls

For the preparation of the side walls, the procedure described in the report "Results of Light Reflectance Measurements from Rough Surfaces"[1] is used. The roughness of the end surfaces, upper and lower walls, which are polished to six hundred grit abrasive paper, is held constant throughout the measurements. The side walls are ground to the various abrasive paper levels and then their roughness is determined optically. The technique for the optical measurements was described in the above report. The walls are then inserted and fastened in the resonator for the Q-value measurements.

Q-Value Measurements

The Q-value of the resonator is measured for two cases. First, the resonator is assembled as a conventional rectangular cavity. Next it is assembled with a dielectric strip inserted creating a closed H-guide resonator. The dielectric strip is supported by small blocks of foam material having a dielectric

constant near that of air and practically no losses. The small blocks, approximately 5mm by 2mm by 1.5mm, are located and attached to the end walls of the resonator. They keep the dielectric strip at the center of the circular coupling iris. The effect of the blocks was found to be negligible. The basic technique for the Q-value measurements was described in the report "An Improved Q-Value Measurement Technique".[2] The Q-value of both, the closed H-guide and the conventional resonator, was measured for various degrees of side wall roughness.

Discussion of Measurements and Their Results

For the measurements the TE_{109} mode is selected. This mode has currents flowing only across the upper and lower wall connections. The closed H-guide has then the additional advantage of decreasing field strength values at the upper and lower walls. This results in a considerable reduction of the losses at the connection of the side walls to the upper and lower walls and gives improved repeatability of the measurements. The resonant frequency is 35.2 GHz for the conventional and 34.6 GHz for the closed H-guide resonator.

In the frequency range above 10 GHz energy absorption due to the water vapor is appreciable. One maximum occurs near 26 GHz and the magnitude of signal attenuation becomes dependent on the humidity. For this reason and for the elimination of oxidation, the various walls and associated system components are kept dry in a nitrogen-filled glass jar. The cavity is filled with dry nitrogen for the measurements.

The Q-values for each set of side walls are plotted as a

function of the spread of the reflectance curves. The spread is taken as the angular displacement between the points where the photomultiplier reads six-tenths of the maximum light amplitude. The relationship between the spread and the surface parameters is not yet established. A typical reflectance curve is shown in Fig. 2. Figure 3 illustrates two sets of data, one taken for the conventional resonator, the other with a dielectric strip of lucalox inserted into the cavity. Since the spread of the reflectance curves is a relative measure of the surface roughness, the measurements indicate that the Q-value of the resonator decreases with increasing roughness.

Two observations were made: The scatter of the data is more pronounced for the conventional resonator and the difference between the two sets of data are larger for the conventional resonator. The scatter is smaller for the H-guide resonator due to the reductions of the effects of the connections at the upper and lower walls. Although precautions are taken to reduce this effect, deviations at the torquing of screws to specified values and deviations at aligning the walls cause small errors. The difference in the sets of data can possibly be explained by a difference in the condition of the air on the days of the measurements. To reduce such possibilities, the later measurements were made with dry nitrogen in the resonator. Results of a normalization of data with regard to the low roughness values are shown in Fig. 4. The diagrams illustrate the pronounced trend due to surface roughness. There exists at present a large discrepancy of the theoretical (based on the bulk value of DC conductivity)

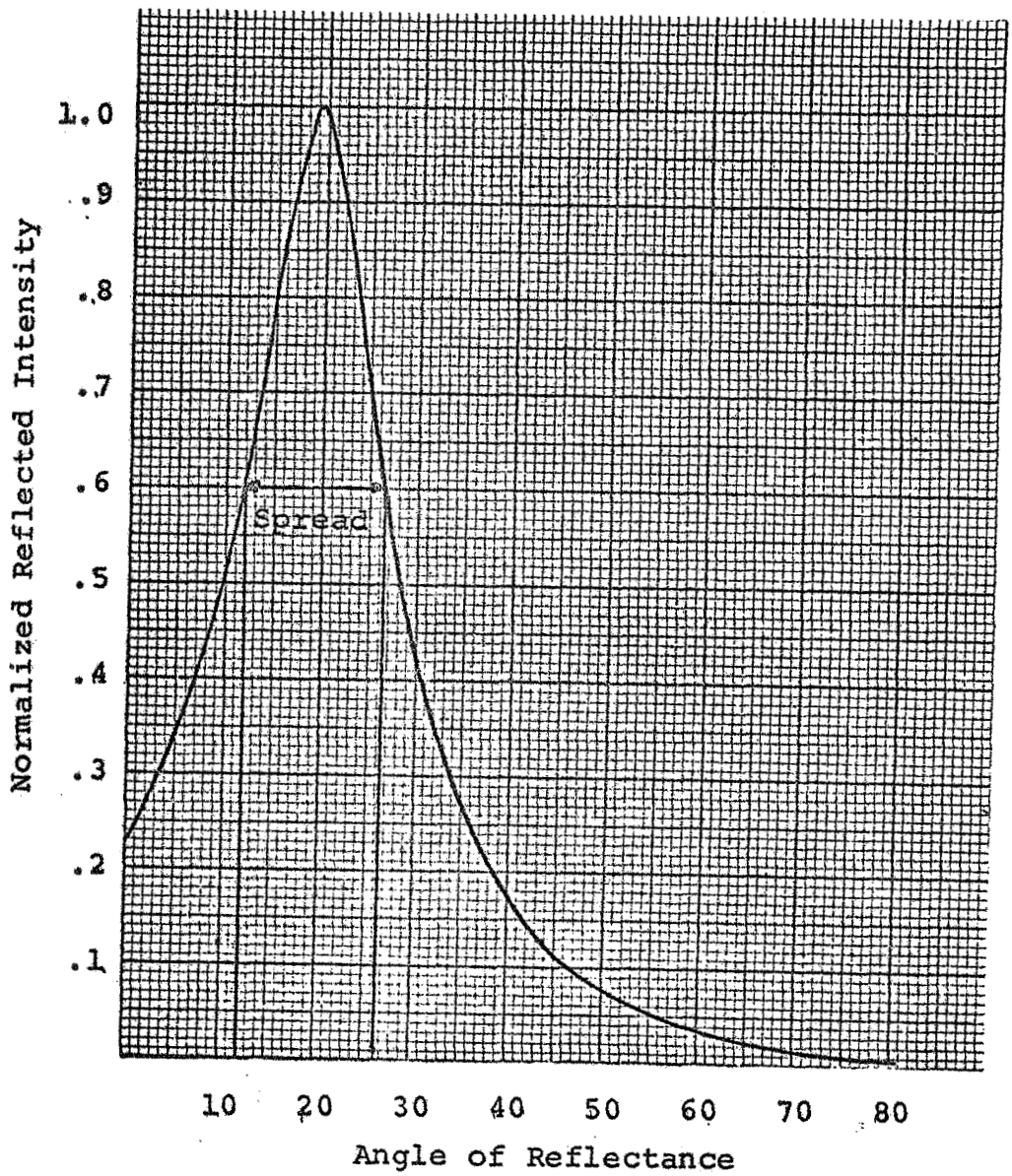

Fig. 2 Typical reflectance curve from a rough surface.

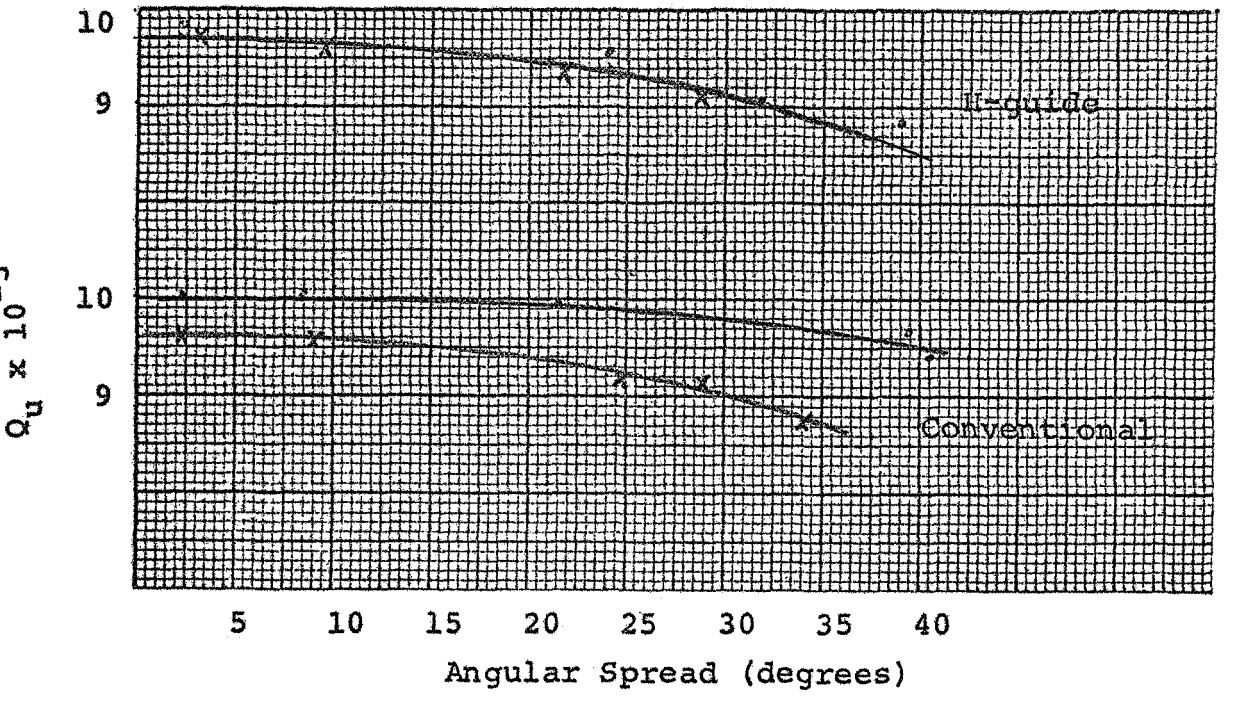

Fig. 3 Unloaded Q vs. angular spread for the closed H-guide and conventional resonator.

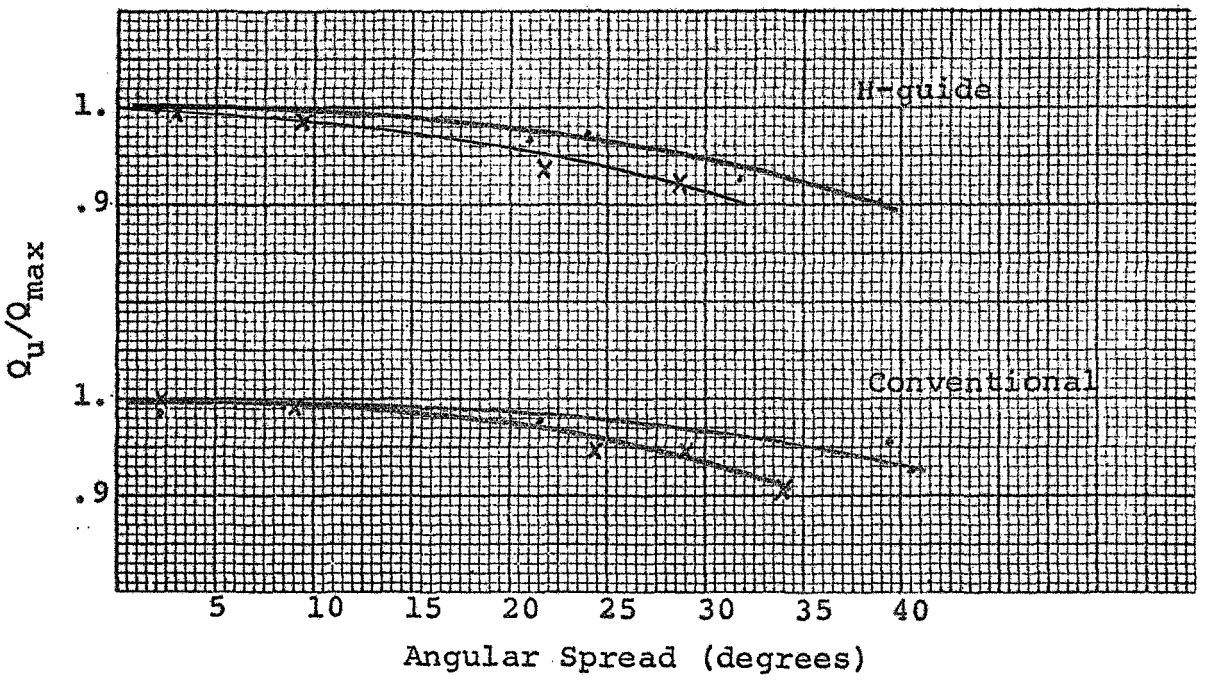

Fig. 4 Normalized Q vs. angular spread for the closed H-guide and conventional resonator.

and the measured Q-values. This effect is at present under investigation.

References

1. L. C. Adair: Results from Light Reflectance Measurements from Rough Surfaces, Progress Report, Grant NGL 34-002-047, pp. 13-30 (June 15, 1970).

2. L. C. Adair, R. A. Kraft: An Improved Q-Value Measurement Technique, Progress Report, Grant NGL 34-002-047, pp. 31-39 (June 15, 1970).

MEASUREMENTS ON MICROSTRIP LINES

Abstract

The propagation characteristics at millimeter wavelengths of microstrip transmission lines are discussed. The results of an experimental investigation of the properties of strip lines on alumina substrates in the frequency range of 31-35 GHz are reported.

Introduction

A microstrip transmission line consists of a metal strip and a ground plane separated by a dielectric slab as shown in Fig. 1. This configuration has become a popular alternative to classical shielded transmission lines due to its adaptability to mass production of integrated microwave circuits.

The electrical quantities of microstrip lines that are important for circuit design are the impedance, the guide wavelength λ_g, the propagation constants α and β, and the unloaded quality factor Q_u of shorted sections. Although microstrip cannot support propagation of pure TEM modes due to the dielectric interface, TEM assumption appears to be a good first-order approximation. Under this assumption, Wheeler[1] established relations between the above parameters, the geometry of the microstrip line, and the effective dielectric constant ε_r' of the dielectric.

The value of ε_r' , the properties of the conductor and substrate materials, and the operational frequency determine the transmission characteristics of the line. The equations

governing these parameters, assuming a strip of negligible thickness are:

$$Z_o = Z_{o1}/\sqrt{\varepsilon_r'} \qquad (1)$$

$$\lambda_g = \lambda_o/\sqrt{\varepsilon_r'} \qquad (2)$$

$$\varepsilon_r' = 1 + q_e(\varepsilon_r - 1) \qquad (3)$$

where

Z_{o1} = free space characteristic impedance

and q_e = effective filling factor.

Using the above equations, it can be shown that for a line of a characteristic impedance of 50 ohms on an alumina substrate and of a geometry ratio w/h = 1, the effective dielectric constant is $\varepsilon_r' = 6.25$ and the guide wavelength $\lambda_g = 0.364$ cms at 33 GHz.

Wheeler's theory is valid only for the case of TEM wave propagation. For this theory to be valid the transverse dimensions of the microstrip (w or h) should be considerably less than $\lambda_g/4$. Otherwise both TE and TM surface waves may affect the wave transmission.

Attenuation

The microstrip attenuation is caused by conductor and dielectric losses. These losses may be approximately computed by assuming a uniform current distribution across the width of the strip and also assuming that the ground plane current is distributed uniformly under the conductor.

The average power flowing through the entire cross-section is given by

$$P_t = 1/2(\varepsilon/\mu)^{1/2} \int |E|^2 dA,$$

where dA is an element area of the cross section.

Assuming that the losses per unit length are small and that α is the attenuation constant, the transmitted power is

$$P(z) = P_o e^{-2\alpha z},$$

where z is the direction of propagation, parallel to the strip conductor and P_o is the transmitted power at z = 0. Assuming that the attenuation is caused by conductor and dielectric losses only, α can be expressed as

$$\alpha = \alpha_{c1} + \alpha_{c2} + \alpha_d,$$

where α_{c1} and α_{c2} are the attenuation constants due to the conductors and α_d due to the dielectric.

Then,

$$\alpha = \frac{-dP/dz}{2P(z)} \simeq \frac{P_{c1} + P_{c2} + P_d}{2P(z)} \text{ nepers/unit length},$$

$$\alpha_d = \frac{P_{c1} + P_{c2}}{2P(z)} \simeq \alpha_{c1} + \alpha_{c2} \text{ and } \alpha_d = \frac{P_d}{2P(z)},$$

where P_{c1}, P_{c2} and P_d are the average conductor and dielectric power losses per unit length, and $P(z) \simeq P_t$.

The average power P_c dissipated in the conductor per unit length is given by

$$P_c = \frac{R_s}{2Z_o} \int |E|^2 dl,$$

where $R_s = \sqrt{\pi f \mu / \sigma_c}$ and dl is a length element along the conductor boundary in transverse direction. The power loss in the dielectric per unit length is

$$P_d = 1/2\ \sigma_d \int |E|^2 dA\ ,$$

evaluated over the dielectric portion of the cross section. Since P_d and P_t have the same region of integration, we have

$$\alpha_d = \frac{\sigma_d}{2}\sqrt{\frac{\mu}{\varepsilon}}\ , \qquad (4)$$

which can be seen to be independent of the geometry of the conductor. The conductivity σ_d can be obtained from the complex dielectric constant($\sigma_d = \omega \varepsilon_0 \varepsilon_r''$).

For a low loss dielectric such as alumina, the dielectric losses are very small and can be neglected. Hence, if the conductor materials of the ground plane and the microstrip are the same, we find

$$\alpha \approx \frac{P_{c1} + P_{c2}}{2P} = \frac{P_c}{P} = \frac{R_s}{Z_0 W} \quad \text{nepers/unit length} \qquad (5)$$

where σ_c is the conductivity in mho/m and R_s is the surface resistance. Using the above expression it can be shown that the expected losses at 33 GHz for a copper strip of width and height is 0.129 dB/cm.

In practical cases, however, the current distribution is far from uniform particularly for the case of low values of W/h. Because of the mathematical complexities, exact expressions for the current distribution for practical cases are not readily accessible. In view of the lack of these data Pucal et al[2,3]

adopted a different approach based on a so-called "incremental inductance rule" for calculating the losses for the case of a nonuniform current distribution and claim good agreement between theory and experiment. On the other hand, good agreement between predicted losses based on a theory with uniform current distribution and measured values is also reported.[4,5]

Attenuation Measurements

The measurement of attenuation above 30 GHz requires a low-loss transition from waveguide to the microstrip line. For this purpose a four-step ridged transformer was designed to transform the waveguide impedance to that of microstrip. A thin beryllium copper strip was connected to the ridge waveguide. The design procedure outlined in references 6 and 7 was used to compute the desired impedance at each step and the mechanical dimensions. The height of the last step was selected such that the dielectric hits and stops against the ridge. The mechanical arrangement is shown in Figures 2 and 3.

For the determination of the insertion losses of the transformers, two identical transformers were capacitively connected back to back. This permitted the adjustments of the coupling capacitance for obtaining maximum output at a number of frequencies. The results of the measurement of the attenuation versus frequency are shown in Fig. 4.

The attenuation constant of a microstrip line of the following specifications was determined next.

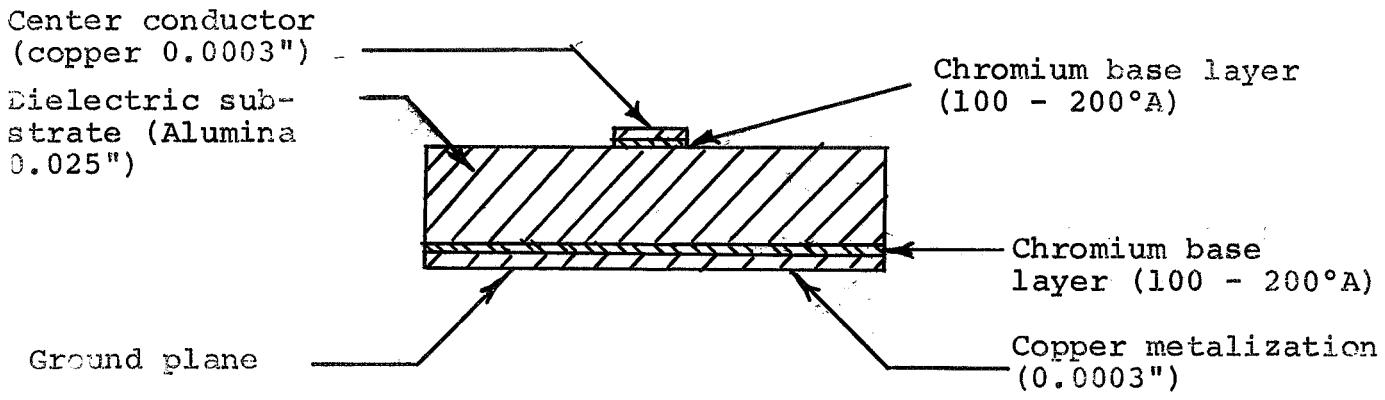

Fig. 1

Fig. 1 Microstrip (sectional view).

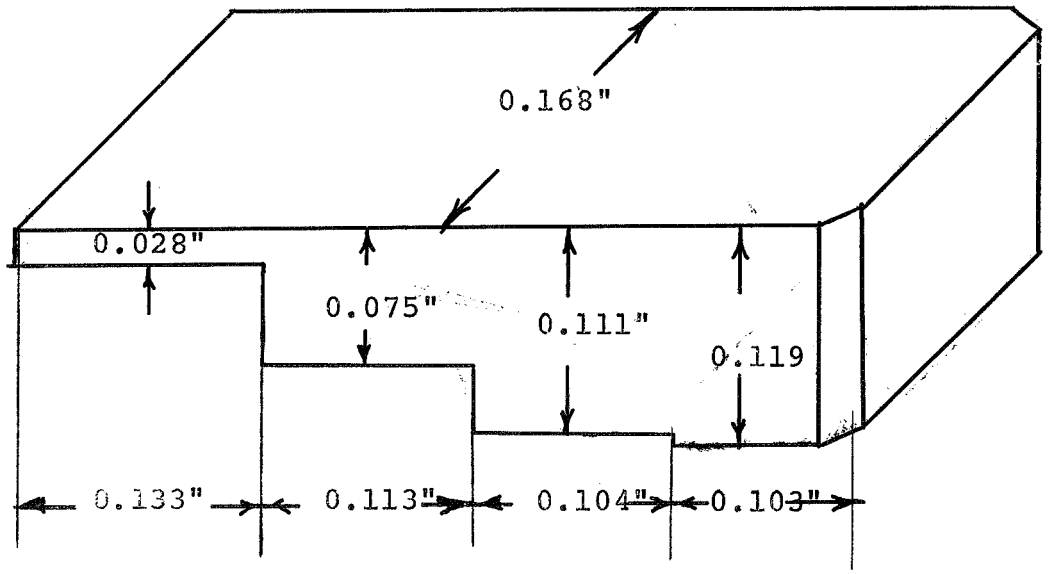

Fig. 2(a)

Fig. 2 Ridge transformer.

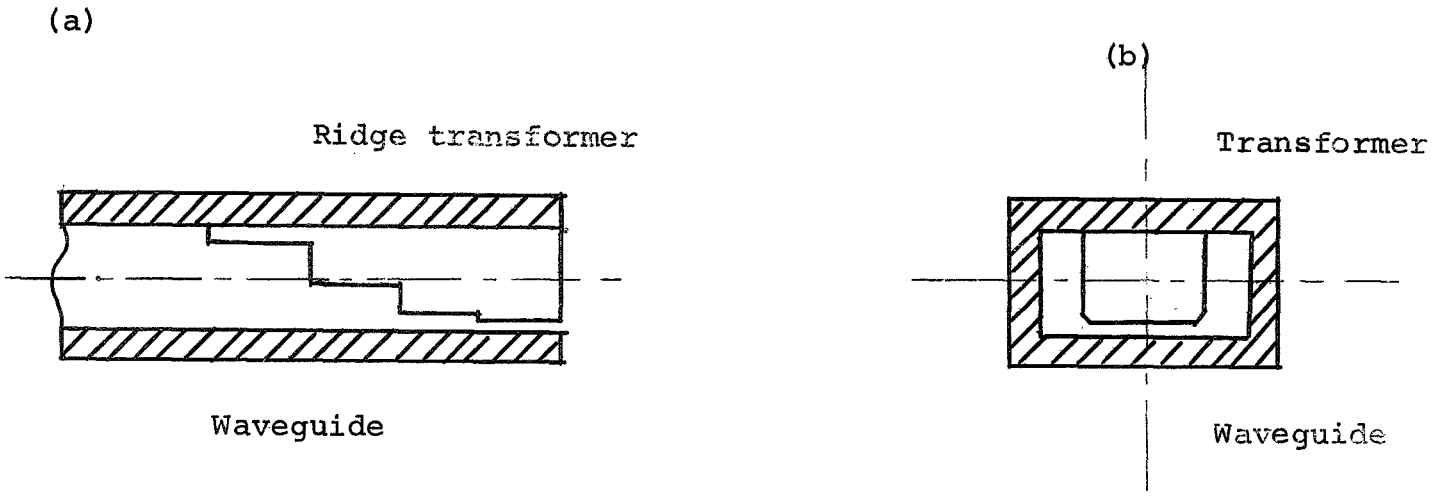

Fig. 3 Waveguide with transformer.
(a) Sectional view.
(b) End view.

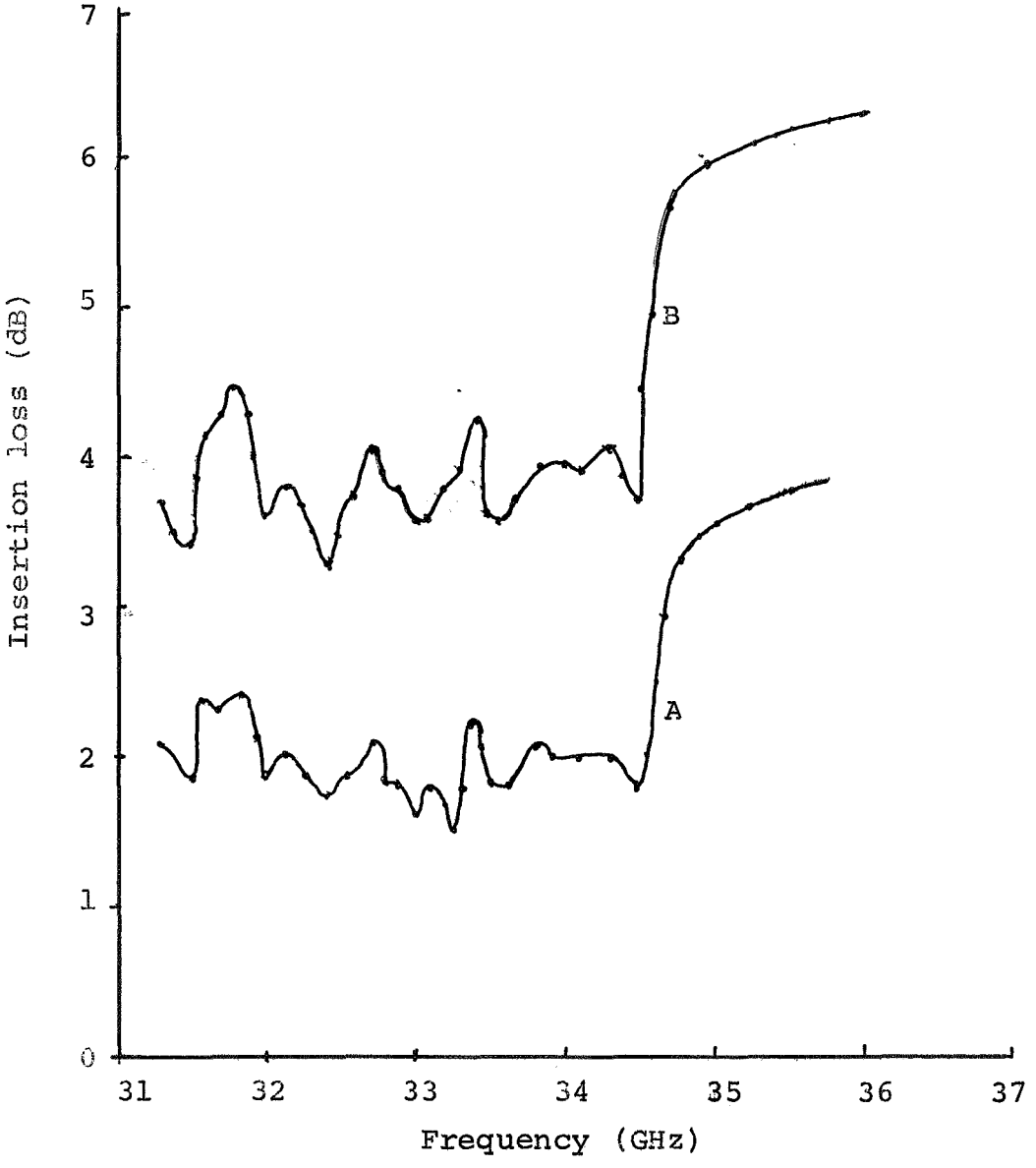

Fig. 4 Measured insertion loss vs. frequency of ridge transformer and microstrip.

A Transformer only.
B Transformer and line.

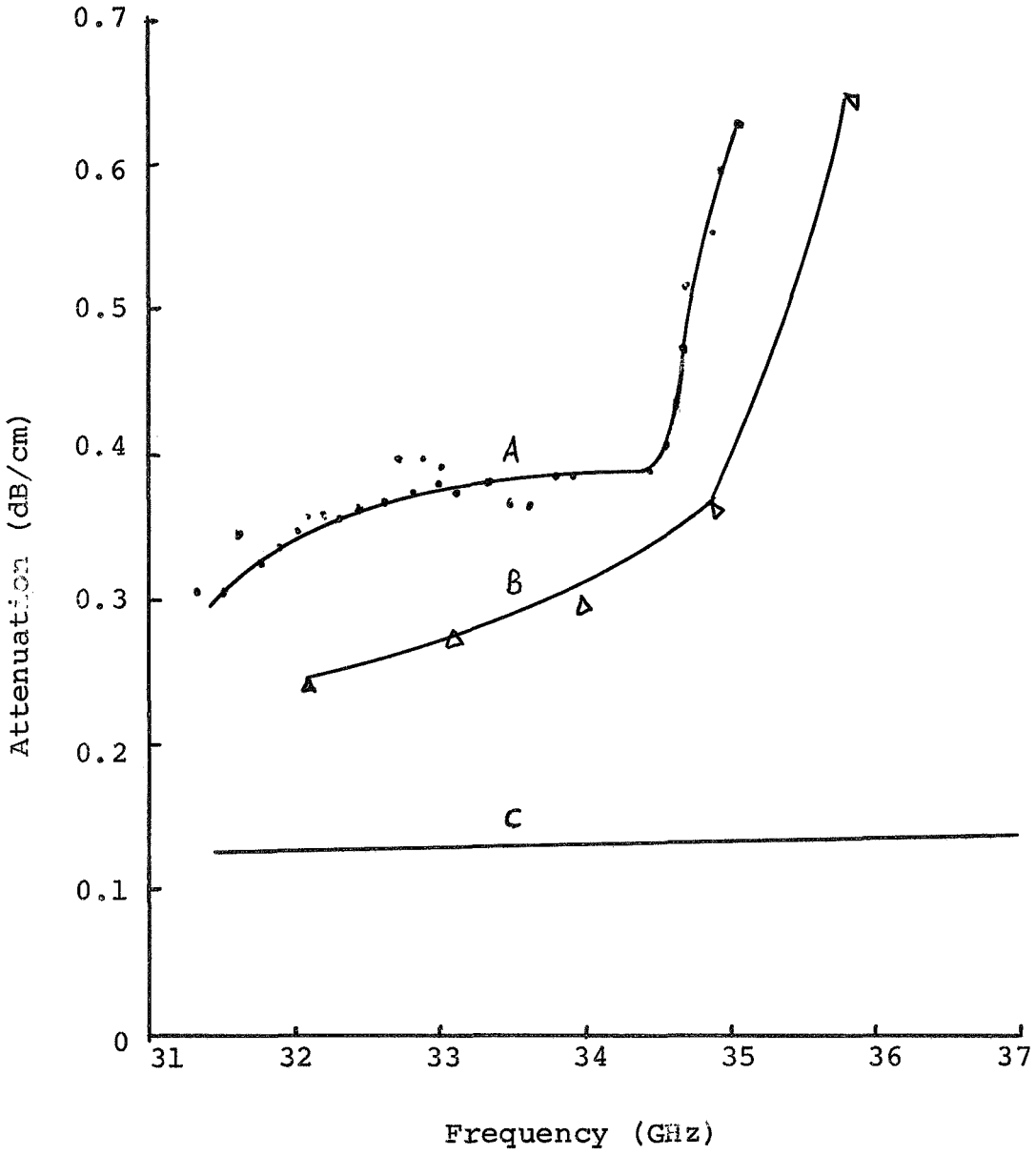

Fig. 5a Attenuation vs. frequency of microstrip line.
A From insertion loss measurements.
B From Q-value measurements.
C Theoretical relationship.

Microstrip data:

Substrate material	99.5% alumina
Substrate thickness	0.025 in.
Substrate finish	2 microinches
Dielectric constant	9.3-9.7 (quoted value at 10 GHz)
Loss tangent	0.0001 (quoted value at 10 GHz)
Conductor material	Copper
Conductor width	0.025 in.
Conductor thickness	0.0003 in.
Base layer	chromium
Base layer thickness	100-200 Å
Line length	2 in.

For determining the total insertion loss (including the line), the energy was capacitively coupled to the line at the input and output ports. The coupling was easily adjustable by varying the gap between the connecting tab and the line and also by moving the line laterally by a small amount. In measuring the insertion loss, the coupling was adjusted for maxium output at each frequency. From the knowledge of the insertion loss due to the transformers alone, the attenuation of the line was computed. The results are shown in Figs. 4 and 5a.

Q-Value Measurements

The attenuation constant was also computed from Q-value measurements using a shorted section of the microstrip line as a resonator. At these measurements, the microstrip was critically coupled to the connecting waveguides. The critical coupling was preferred as this suppresses spurious resonances produced by mismatches. An added advantage of this coupling was that it was easily monitored on the oscilloscope. Also, for this coupling, the unloaded quality factor is simply twice the loaded quality factor. The Q-value of the resonator was

evaluated from the VSWR measurements at several frequencies on either side of resonance. It can be easily shown that the Q and the VSWR are related by the equation,

$$\left(S+\frac{1}{S}\right) = S_o+\frac{1}{S_o} + \left[\frac{S_o+1}{\sqrt{S_o}} \cdot \frac{2Q_L}{f_o}\right]^2 (f-f_o)^2 ,$$

where S is the VSWR at any frequency f and S_o is the VSWR at resonance frequency. A plot of S + 1/S versus $(f - f_o)^2$ gives a straight line, the slope of which is

$$\left[\frac{S_o+1}{\sqrt{S_o}} \cdot \frac{2Q_L}{f_o}\right]^2$$

From this it can be seen that

$$Q_L = \frac{f_o}{2(1+S_o)} \sqrt{S_o \cdot (\text{Slope})} \qquad (6)$$

Measurement results are shown in Fig. 5b. The coupling condition required for computation of the unloaded Q was obtained by placing a VSWR meter (slotted line) in front of the resonator. The probe of the SWR meter was inserted into the guide and the trace of the reflected power was observed on the scope as the probe distance from the resonator was varied. From the nature of the locus traced, the coupling condition can be obtained. The direction of the travel of locus traced out is clockwise for the overcoupled case and the opposite for undercoupling as the probe moves away from the cavity. In case of critical coupling the movement of the trace is negligible. The values of VSWR were obtained by evaluation of the probe output at several frequencies.

Analyzing the equivalent circuit of this resonator, it

can be shown that the attenuation constant becomes[3]

$$\alpha \approx \frac{4.34\,\beta}{Q_u} \quad [\mathrm{dB/cm}] \qquad (7)$$

where $\beta = 2\pi/\lambda_g$.

The guide wavelength was obtained from field plots along the line using a compensated probe. Two examples of such plots are shown in Fig. 7 and 8. The measured value of λ_g differed only by 5% from the computed values using a value of 6.25 for the effective dielectric constant of alumina.

The results of computed values of attenuation using this method at four different resonant frequencies are shown in Fig. 5a.

Conclusions

The values of guide wavelength computed from the field patterns above the microstrip lines using a compensated probe are in agreement with the predicted values based on Wheeler's theory. It was found that the effective dielectric constant of alumina at 35 GHz is 6.25.

From Fig. 5a, it can be seen that considerable discrepancies exist between the computed losses and the measured losses expressed by the attenuation constants. One probable explanation for this difference is that the actual surface conductivity of copper at 35 GHz is much lower than the DC value of 5.8×10^7 mhos/m used in computing the losses. Also, the assumption of uniform current in practice is far from being true since the geometry ratio of the line used is unity.

As the exact value of the loss tangent for alumina at 35 GHz was not available, a value of 0.0001 was assumed in the computation, which is probably true at X-band. The loss tangent at 30 GHz can be expected to be higher than this value and hence the dielectric losses may be of comparable magnitude to the conduction losses and hence cannot be neglected.

Another effect may be the interaction of surface waves with the TEM microstrip waves. Field measurements on the dielectric did indicate the existence of these surface waves and particularly above 34 GHz. Their level was only about 10 dB below that of the TEM waves on the strip. This may cause higher losses measured above 34 GHz. The interacting surface waves are probably of the TM-type. Further studies of these phenomena are in progress.

Photographs of the strip line and of the reflection-type measurement setup for the determination of the Q-values are shown in Figs. 9 and 10 respectively.

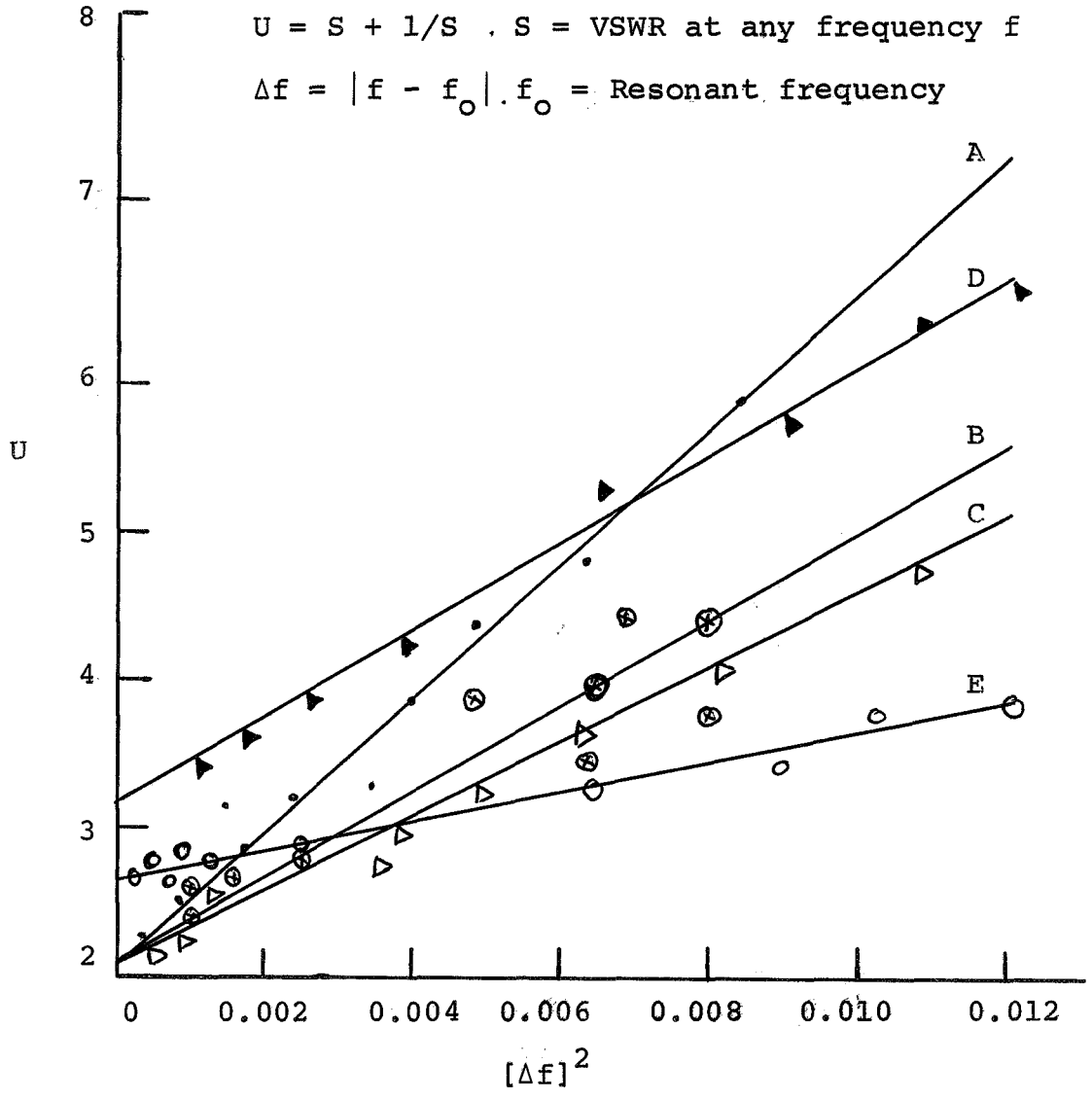

Fig. 5b: Relationship between standing wave ratio and frequency deviation.

	Frequency GHz	Coupling
A	32.1	Under coupling.
B	33.07	Over coupling.
C	33.99	Over coupling.
D	34.9	Under coupling.
E	35.9	Under coupling.

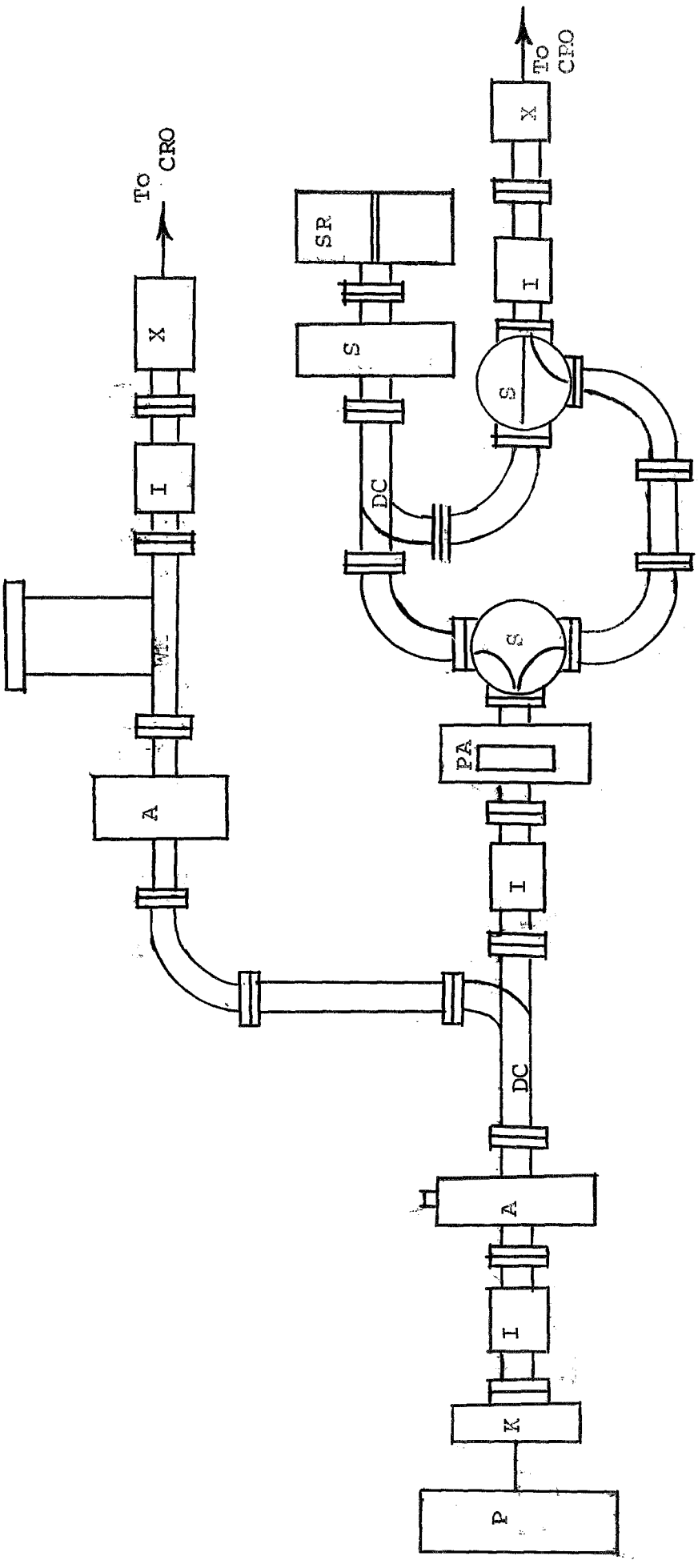

A Attenuator.
DC Directional Coupler.
I Isolator.
K A-band Klystron.
P Power Supply with External Modulator.
PA Precision Attenuator.
S Switch.
SR Stripline Resonator.
X Tunable Crystal.
CM Cavity Wave Meter.

Fig. 6 Setup for measurement of Q-values by evaluation of reflection coefficients.

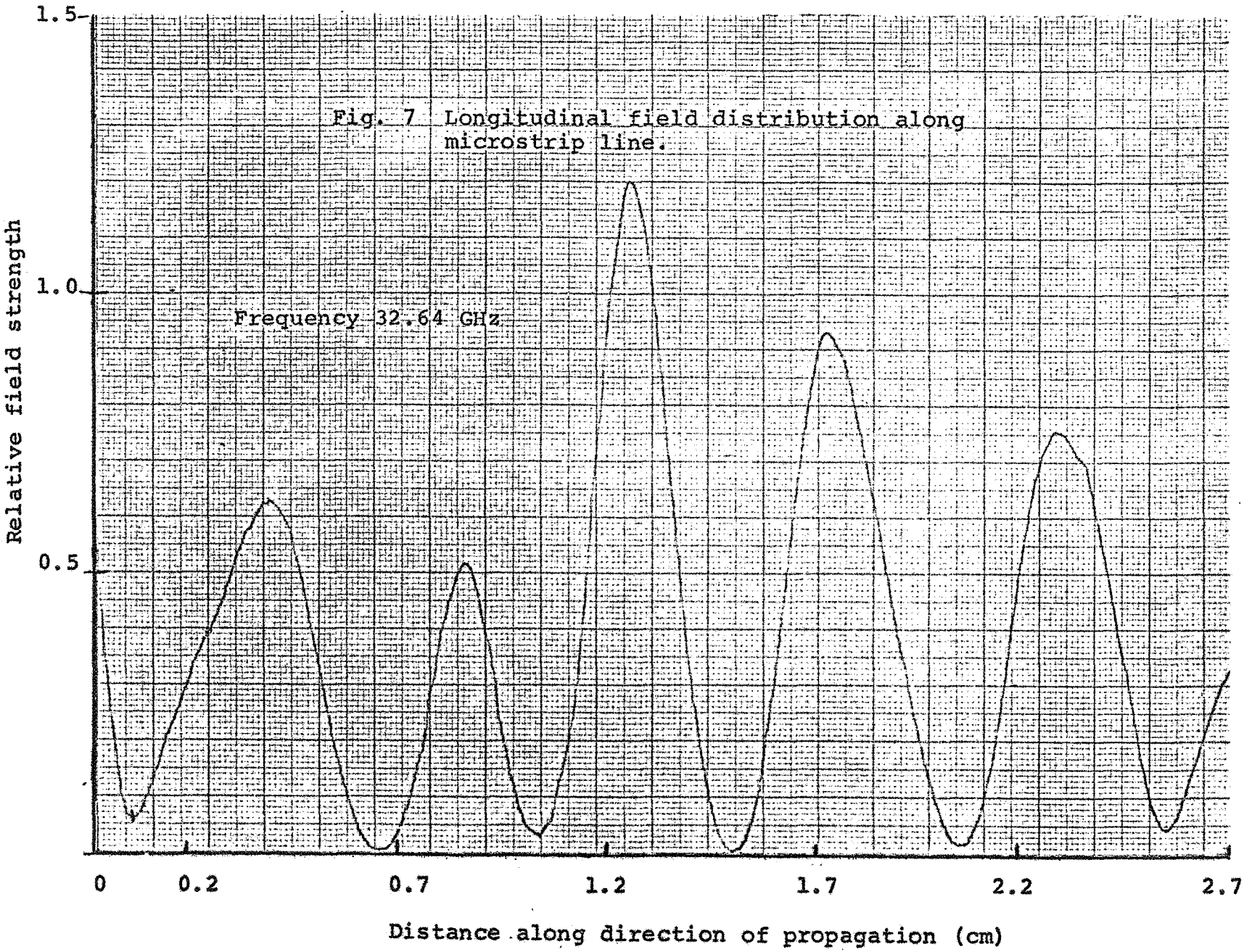

Fig. 7 Longitudinal field distribution along microstrip line.

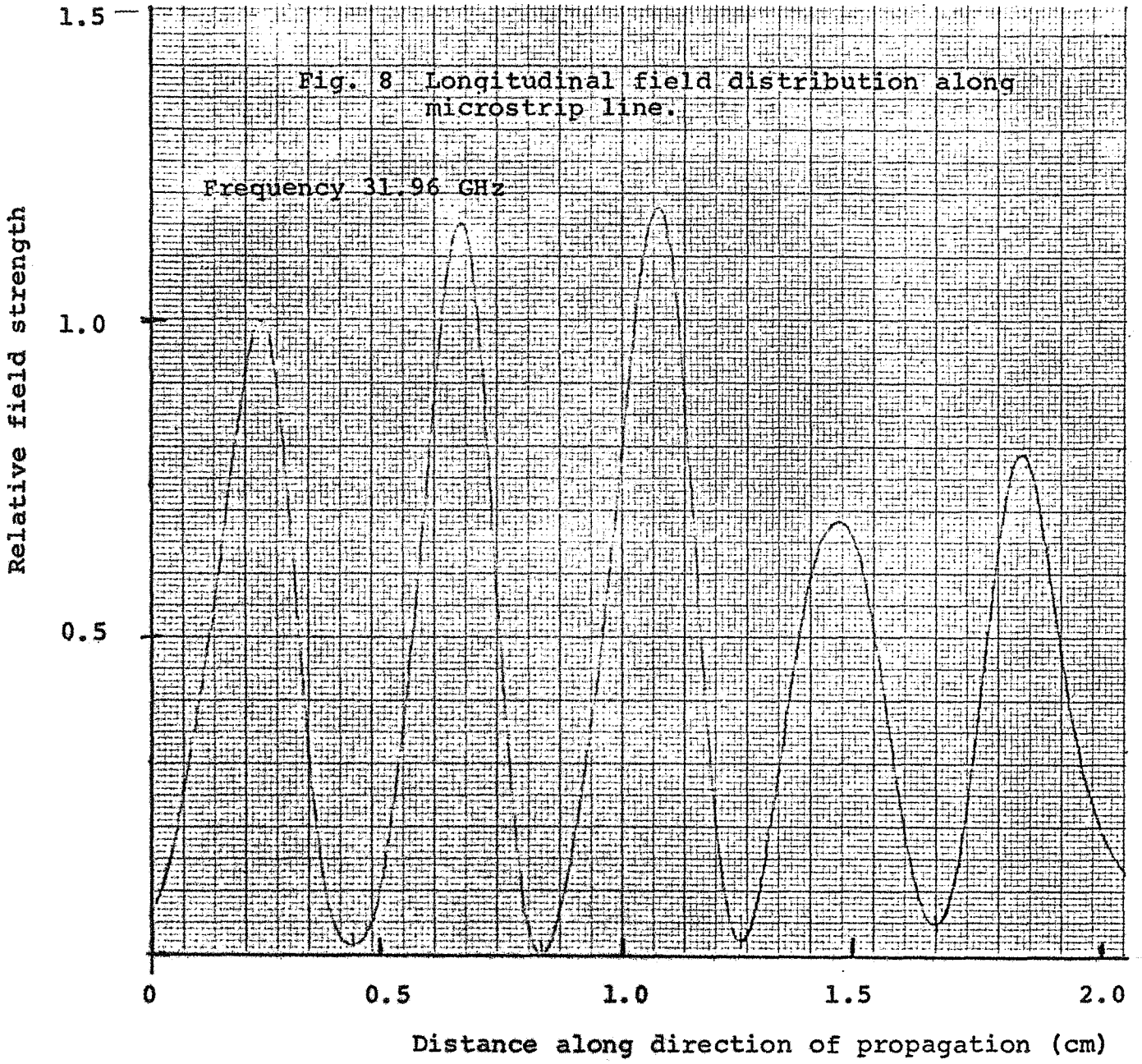
Fig. 8 Longitudinal field distribution along microstrip line.
Frequency 31.96 GHz
Relative field strength
1.5
1.0
0.5
0
0.5
1.0
1.5
2.0
Distance along direction of propagation (cm)

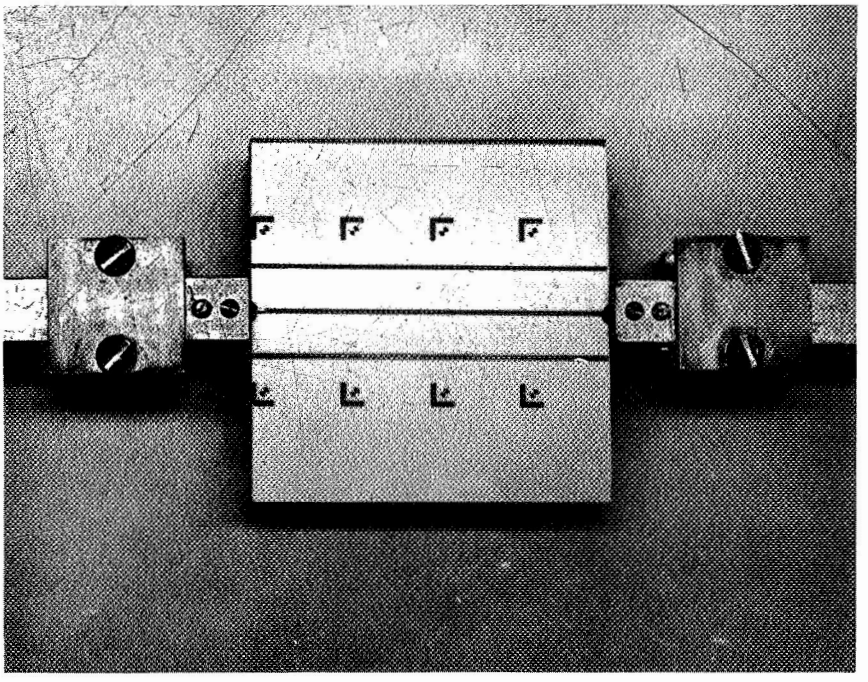

Fig. 9 Microstrip transmission line with connecting waveguides.

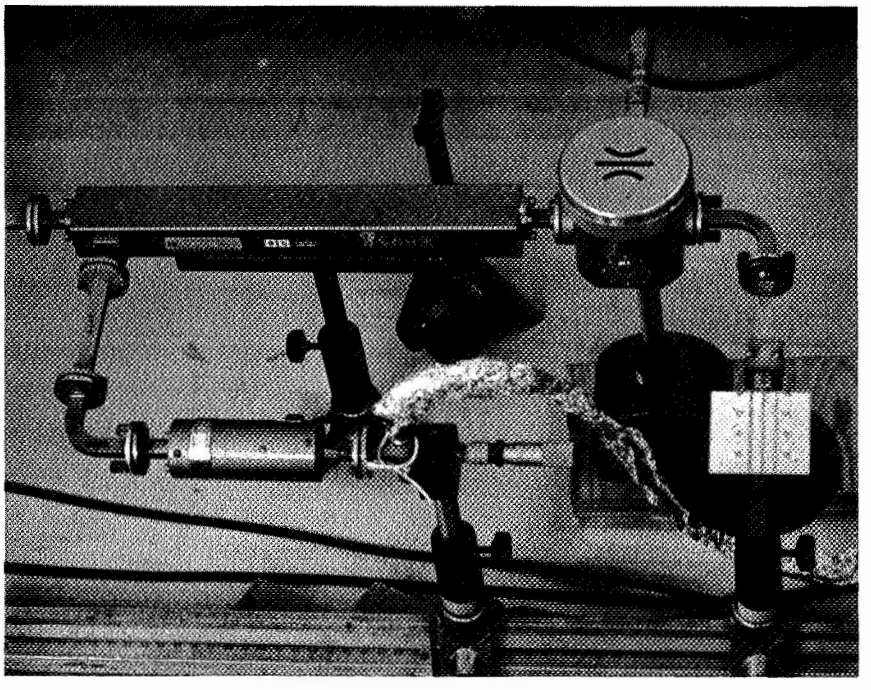

Fig. 10 Reflection-measurement setup for the determination of the Q-value.

References

1. H. A. Wheeler: Transmission Line Properties of Parallel Strips Separated by a Dielectric Sheet, IEEE Trans. on Microwave Theory and Techniques, Vol. MTT-13, pp. 412-424 (March 1965).

2. C. P. Hartwig, D. Masse, and R. A. Pucal: Frequency Dependent Behaviour of Microstrip, presented at the G-MTT International Microwave Symp., Detroit, Michigan (May 20-22, 1968. (referenced in 3).

3. R. A. Pucal, D. J. Masse and C. P. Hartwig: Losses in Microstrip, IEEE Trans. on Microwave Theory and Techniques, Vol. MTT-16, pp. 342-350 (June 1968).

4. M. Caulton, J. J. Hughes and H. Sobol: Measurements on the Properties of Microstrip Lines for Microwave Integrated Circuits, RCA Rev., Vol. 27, pp. 371-391 (1966).

5. M. V. Schneider: Microstrip Lines for Microwave Integrated Circuits, Bell System Technical Journal, Vol. 48, No. 5, pp. 1421-1443 (May, June 1969).

6. S. B. Cohn: Optimum Design of Stepped Transmission Line Transformers, IRE Trans. on Microwave Theory and Techniques, Vol. MTT-3, pp. 16-21 (April 1955).

7. S. Hoffer: The Design of Ridged Waveguides, IRE Trans. on Microwave Theory and Techniques, Vol. MTT-3, pp. 20-29, Oct. 1955.

8. L. Malter and G. R. Brewer: Microwave Q-Measurements in the Presence of Series Losses, Journal of Applied Physics, Vol. 20, pp. 918-925 (October 1949).

9. _____: Handbook of Microwave Measurements, Volume II, edited by M. Sucher and Jerome Fox, Polytechnic Press of PIB, Interscience Publishers, Wiley and Sons, Inc. (1963).